Supporting Information

Hydrophilic (η^6-arene)-ruthenium(II) complexes with P-OH ligands as catalysts for the isomerization of allyl-benzenes and C-H bond arylation reactions in water

Rebeca González-Fernández, Pascale Crochet,* and Victorio Cadierno*

Laboratorio de Compuestos Organometálicos y Catálisis (Unidad Asociada al CSIC), Centro de Innovación en Química Avanzada (ORFEO-CINQA), Departamento de Química Orgánica e Inorgánica, Instituto Universitario de Química Organometálica "Enrique Moles", Facultad de Química, Universidad de Oviedo, Julián Clavería 8, E-33006 Oviedo, Spain

E-mail: crochetpascale@uniovi.es (P.C.); vcm@uniovi.es (V.C.).

Contents

Table S1. Isomerization of estragole (**3a**) into anethole (**4a**) catalyzed by complex **2g**: Screening of different bases. S2

Table S2. Crystal data and structure refinement for complex $[RuCl_2(\eta^6\text{-}C_6H_5CH_2CH_2CH_2OH)\{P(OH)Me_2\}]$ (**2a**). S3

NMR spectra of the ruthenium(II) complexes **2a-g**. S4-S14

NMR spectra of the isolated (1-propenyl)benzene derivatives **4a-k**. S15-S25

^{1}H NMR spectra of the arylation reactions collected in Table 7. S26-S31

Table S1. Isomerization of estragole (**3a**) into anethole (**4a**) catalyzed by complex **2g**: Screening of different bases.[a]

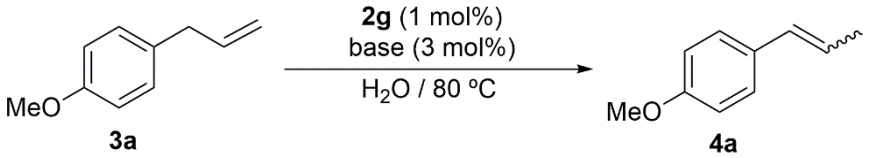

Entry	Base	Time (h)	Yield of **4a** (%)[b]	*E/Z* ratio[b]
1	NaOH	2	86	92:8
		4	98	93:7
		5	> 99	93:7
2	LiOH	2	84	91:9
		4	97	93:7
		5	99	93:7
3	KOH	2	85	92:8
		4	98	93:7
		5	> 99	93:7
4	$CsOH{\cdot}H_2O$	2	87	92:8
		4	97	93:7
		5	> 99	93:7
5	Na_2CO_3	2	83	91:9
		4	96	92:8
		5	> 99	93:7
6	K_2CO_3	2	90	93:7
		4	> 99	94:6
7	Cs_2CO_3	2	85	91:9
		4	98	93:7
		5	> 99	94:6
8	KO^tBu	2	74	91:9
		4	94	92:8
		5	97	93:7

[a] Reactions performed under argon atmosphere using 2 mmol of **3a**, 0.02 mmol of complex **2g**, 0.06 mmol of base and 1 mL of water. [b] Determined by GC (uncorrected GC areas).

Table S2. Crystal data and structure refinement for complex [$RuCl_2(\eta^6$-$C_6H_5CH_2CH_2CH_2OH)\{P(OH)Me_2\}$] (**2a**).

Empirical formula	$C_{11}H_{19}Cl_2O_2PRu$	
Formula weight (g.mol^{-1})	386.20	
Temperature	298(2) K	
Radiation type	Cu Kα	
Wavelength	1.54184 Å	
Crystal system	monoclinic	
Space group	$P2_1/n$	
Unit cell dimensions	a = 8.6015(3) Å	α = 90°
	b = 7.2231(3) Å	β = 97.326(4)°
	c = 23.4552(9) Å	γ = 90°
Volume	1445.4(1) Å^3	
Z	4	
Density (calculated)	1.775	
Absorption coefficient	13.137 mm^{-1}	
F(000)	776	
Crystal size	0.24 x 0.11 x 0.07 mm^3	
Theta range for data collection	3.80 to 69.47°	
Limiting indices	$-10 \leq h \leq 10$, $-5 \leq k \leq 8$, $-24 \leq l \leq 28$	
Reflections collected	6469	
Independent reflections	2678 [R(int) = 0.0368]	
Completeness to theta = 69.47°	98.3 %	
Refinement method	Full-matrix least-squares on F^2	
Data / restraints / parameters	2678 / 0 / 164	
Goodness-of-fit on F^2	1.038	
Final R indices [I > 2sigma(I)][a]	R_1 = 0.0329, wR_2 = 0.0811	
R indices (all data)	R_1 = 0.0386, wR_2 = 0.0854	
Largest diff. peak and hole	0.628 and -1.259 e.Å^{-3}	

[a] $R_1 = \sum(|F_o|-|F_c|)/\sum|F_o|$; $wR_2 = \{\sum[w(F_o^2-F_c^2)^2]/\sum[w(F_o^2)^2]\}^{1/2}$

NMR spectra of the ruthenium(II) complexes 2a-g

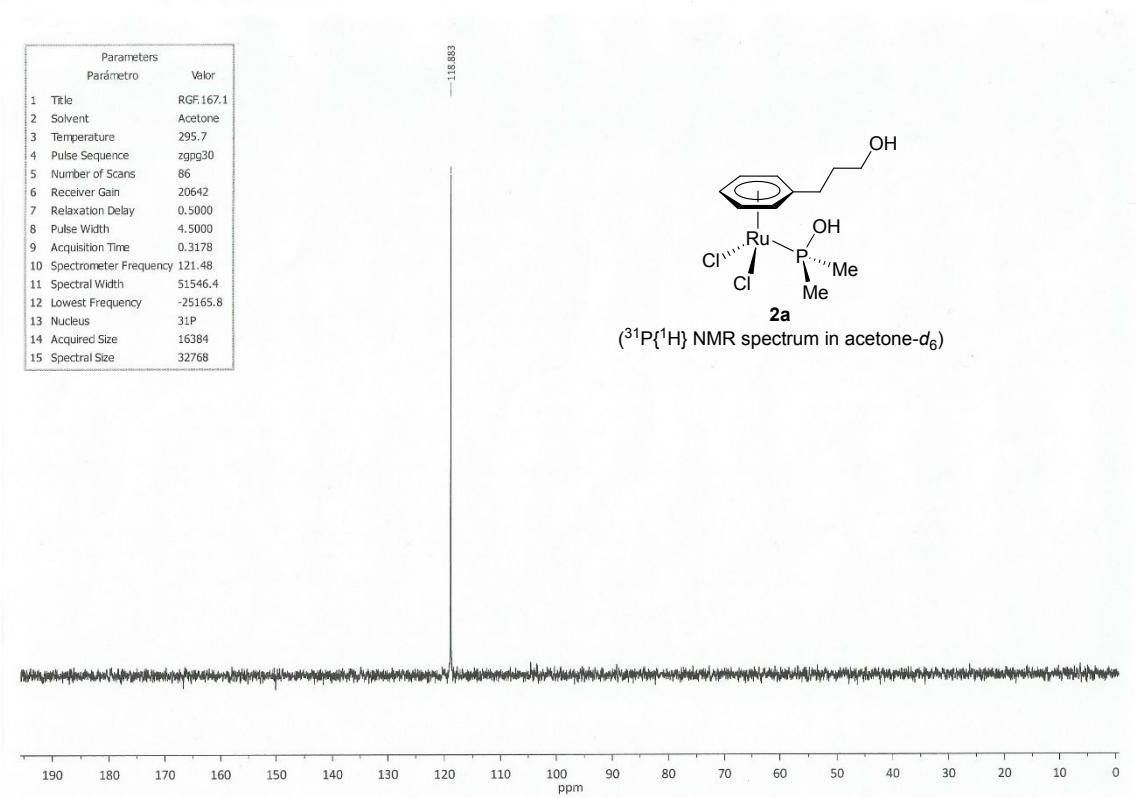

Figure S1: $^{31}P\{^{1}H\}$ NMR spectrum (121 MHz, acetone-d_6) of complex **2a**.

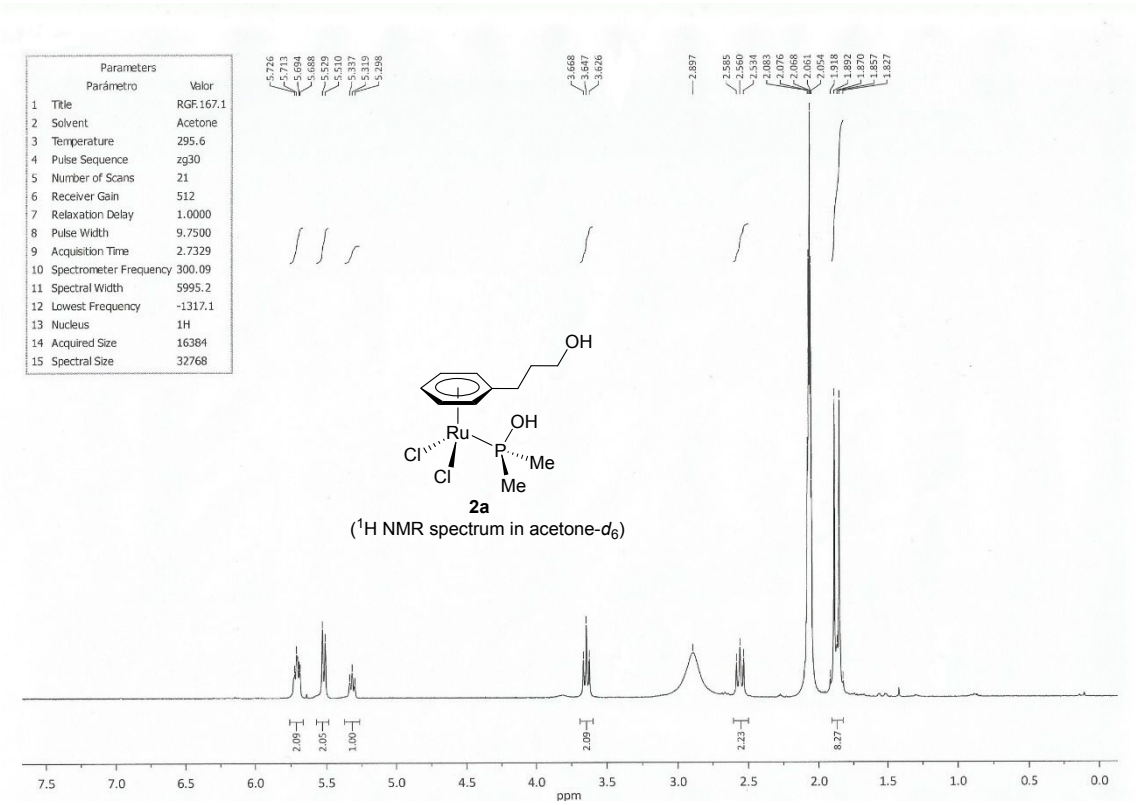

Figure S2: ^{1}H NMR spectrum (300 MHz, acetone-d_6) of complex **2a**.

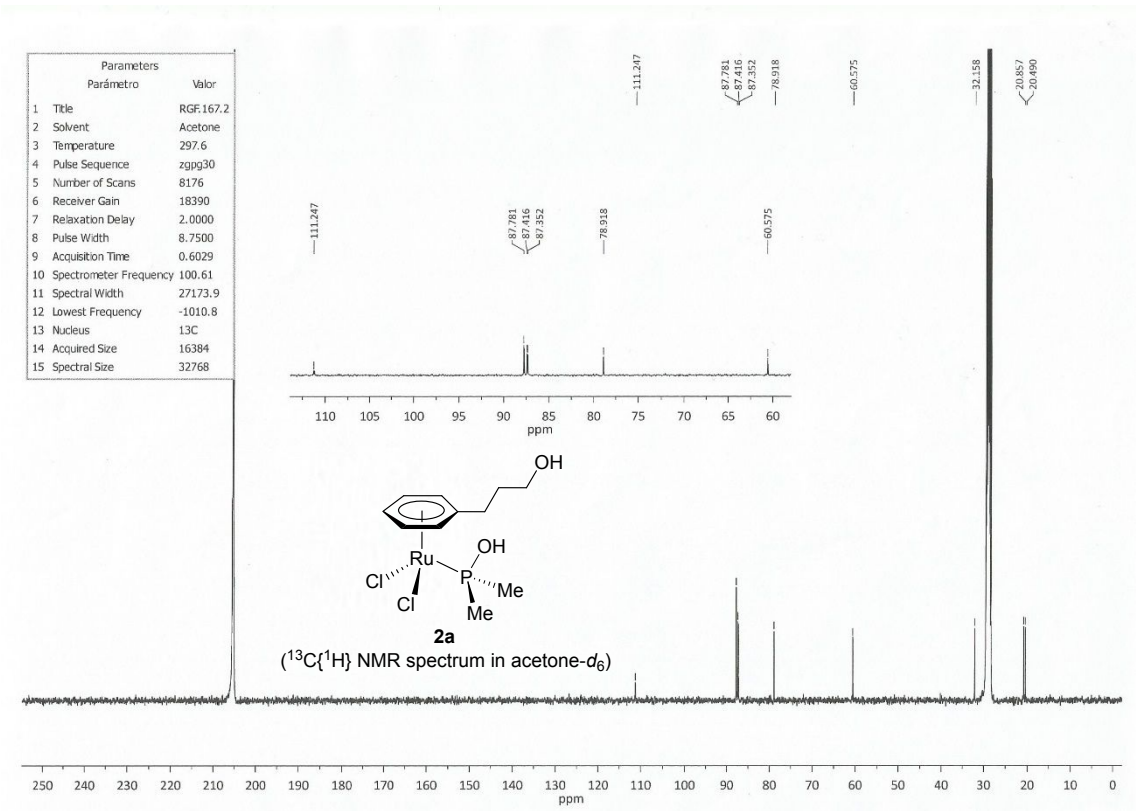

Figure S3: $^{13}C\{^{1}H\}$ NMR spectrum (100 MHz, acetone-d_6) of complex **2a**.

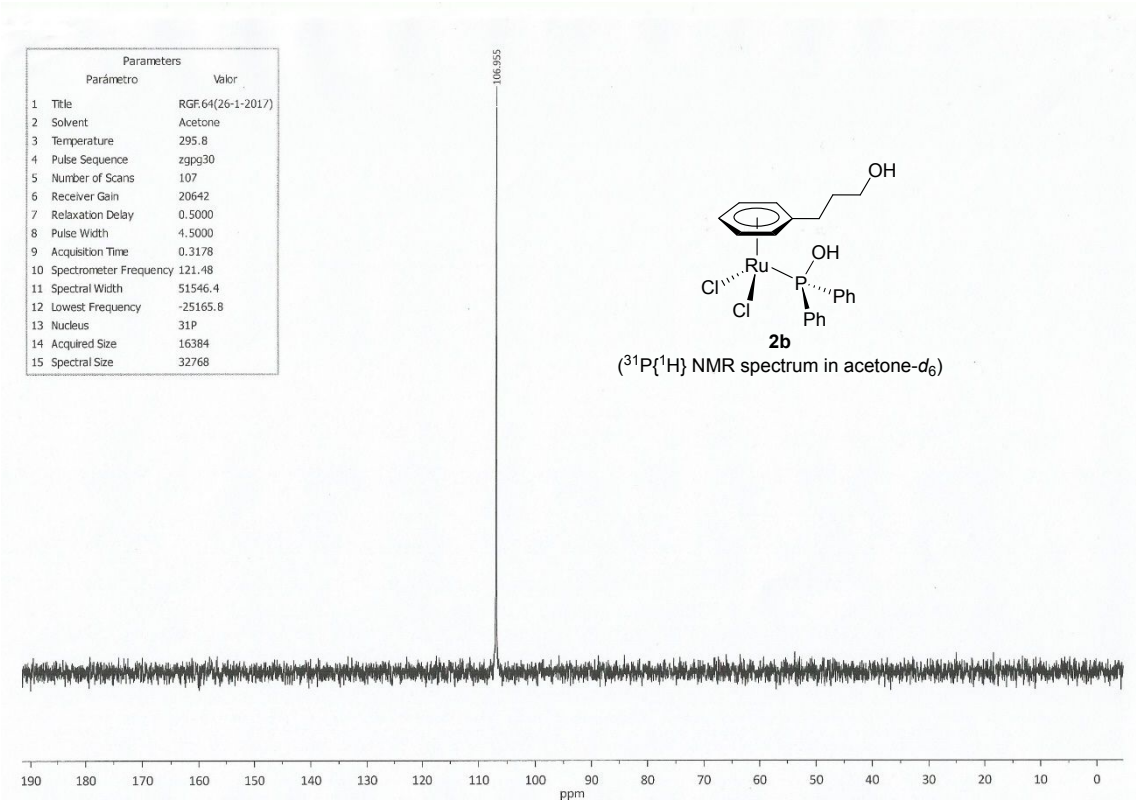

Figure S4: $^{31}P\{^{1}H\}$ NMR spectrum (121 MHz, acetone-d_6) of complex **2b**.

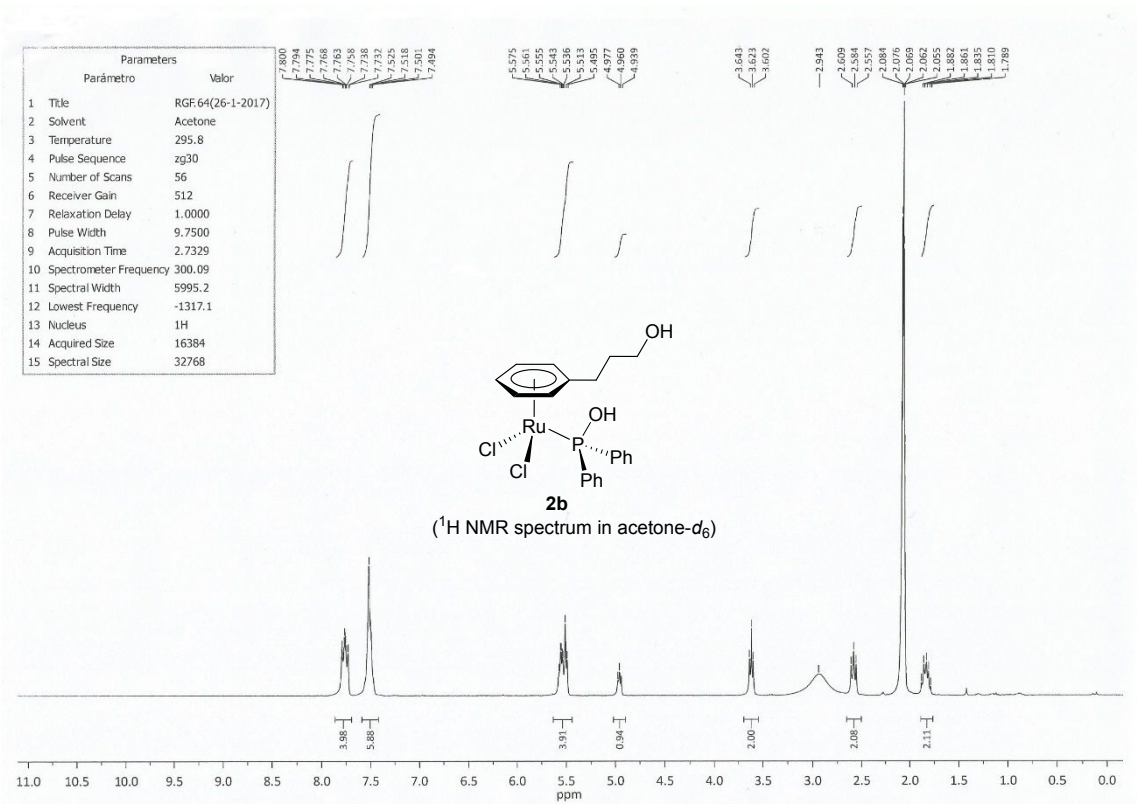

Figure S5: ^{1}H NMR spectrum (300 MHz, acetone-d_6) of complex **2b**.

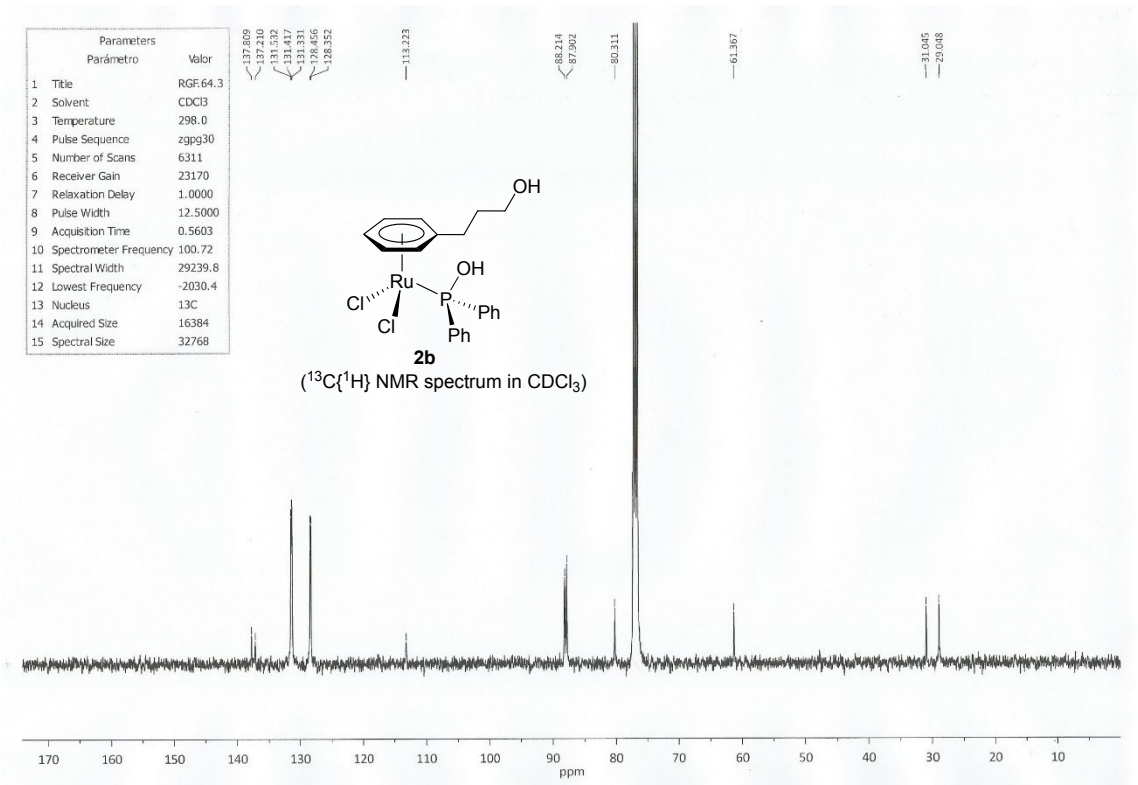

Figure S6: ^{13}C{^{1}H} NMR spectrum (100 MHz, $CDCl_3$) of complex **2b**.

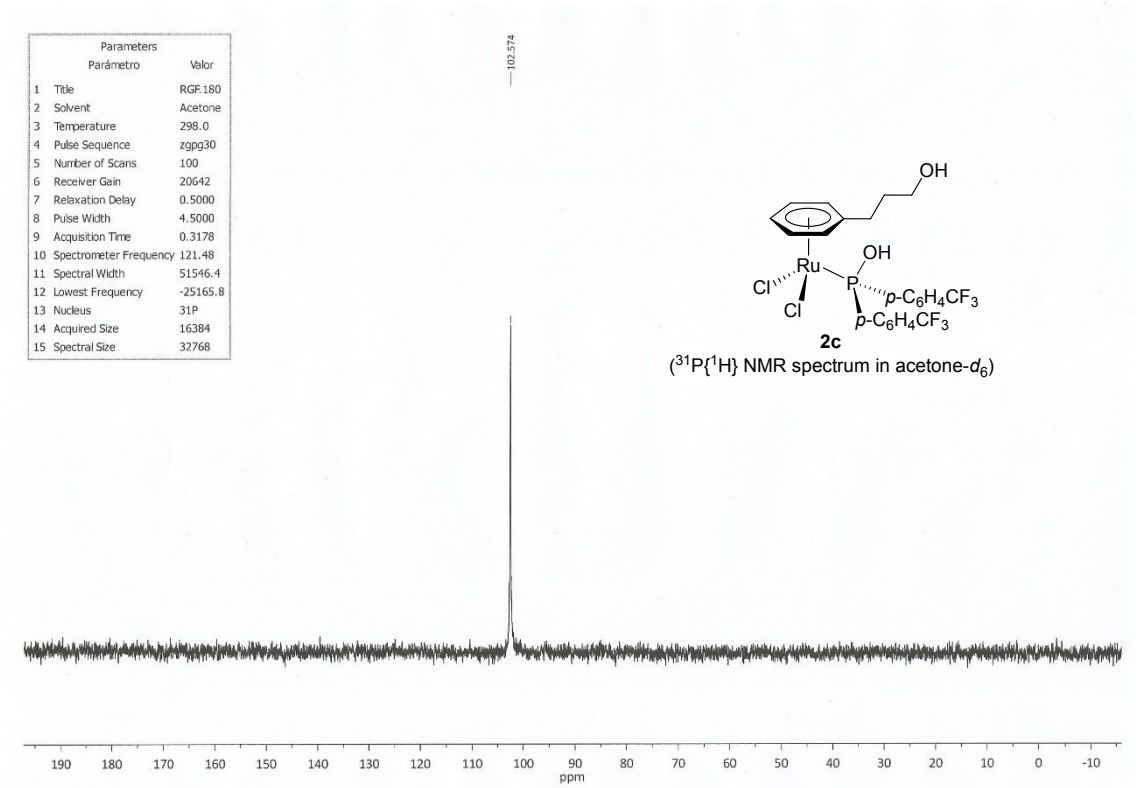

Figure S7: $^{31}P\{^{1}H\}$ NMR spectrum (121 MHz, acetone-d_6) of complex **2c**.

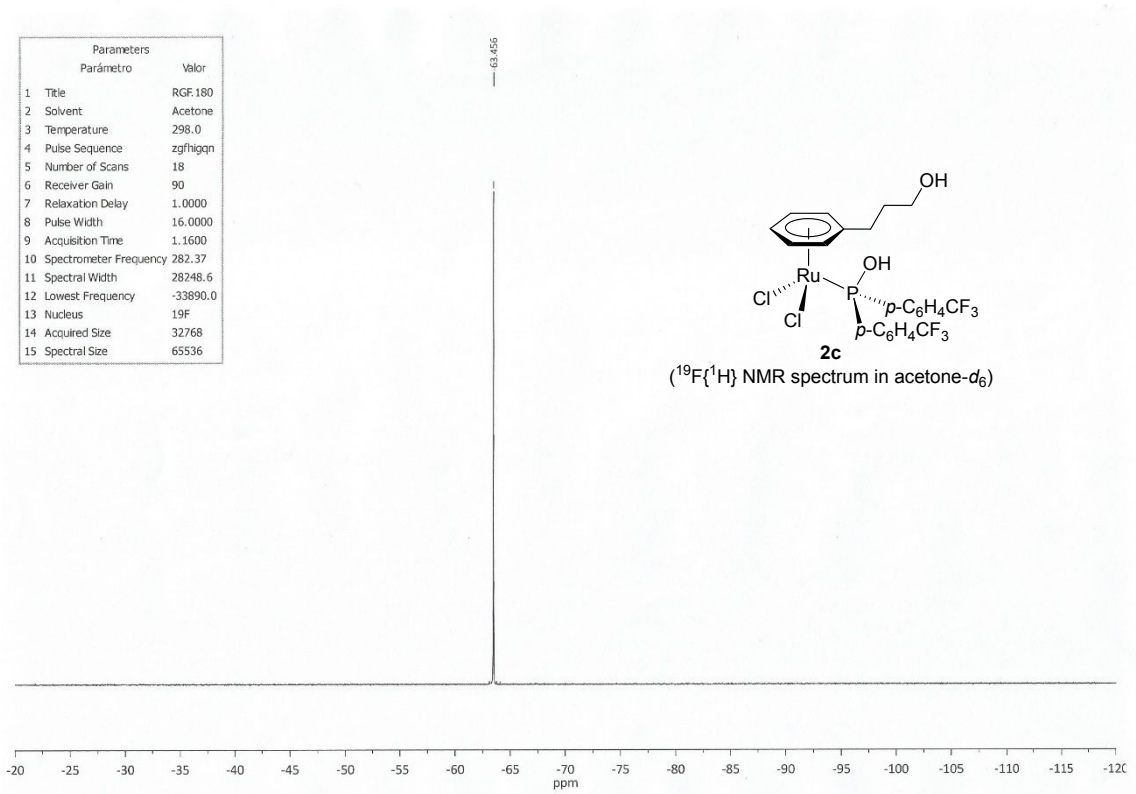

Figure S8: $^{19}F\{^{1}H\}$ NMR spectrum (282 MHz, acetone-d_6) of complex **2c**.

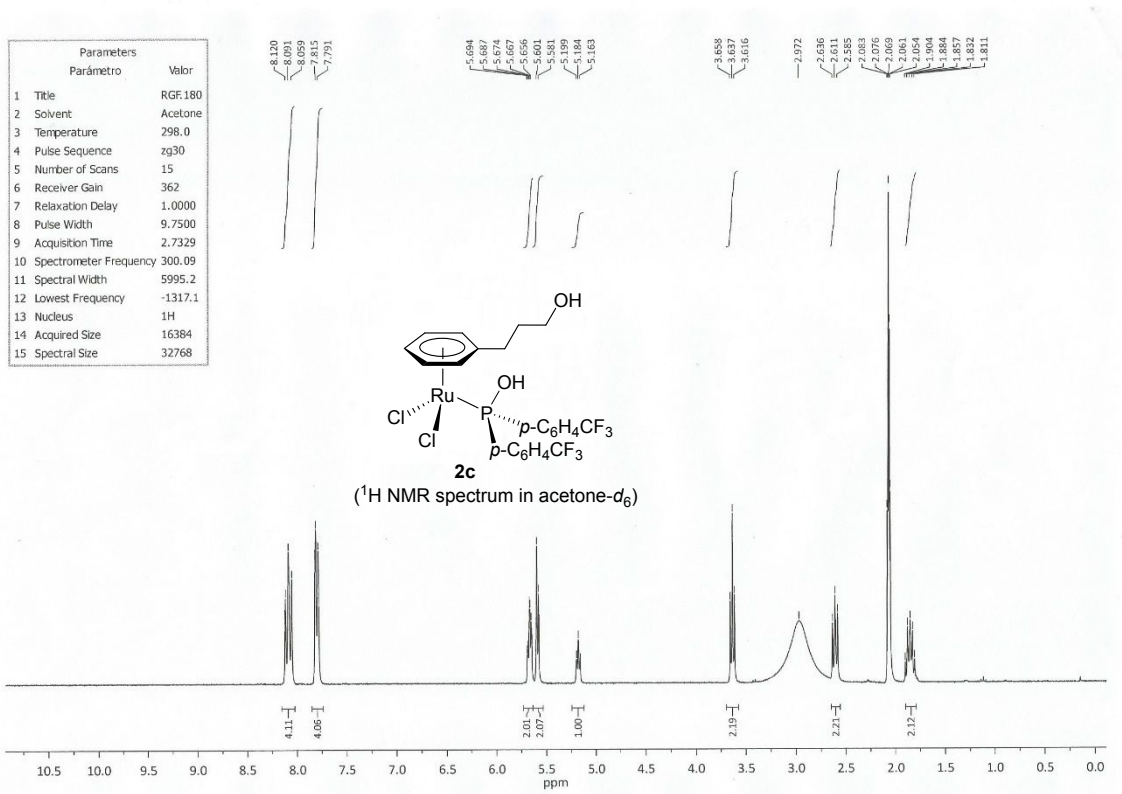

Figure S9: ^{1}H NMR spectrum (300 MHz, acetone-d_6) of complex **2c**.

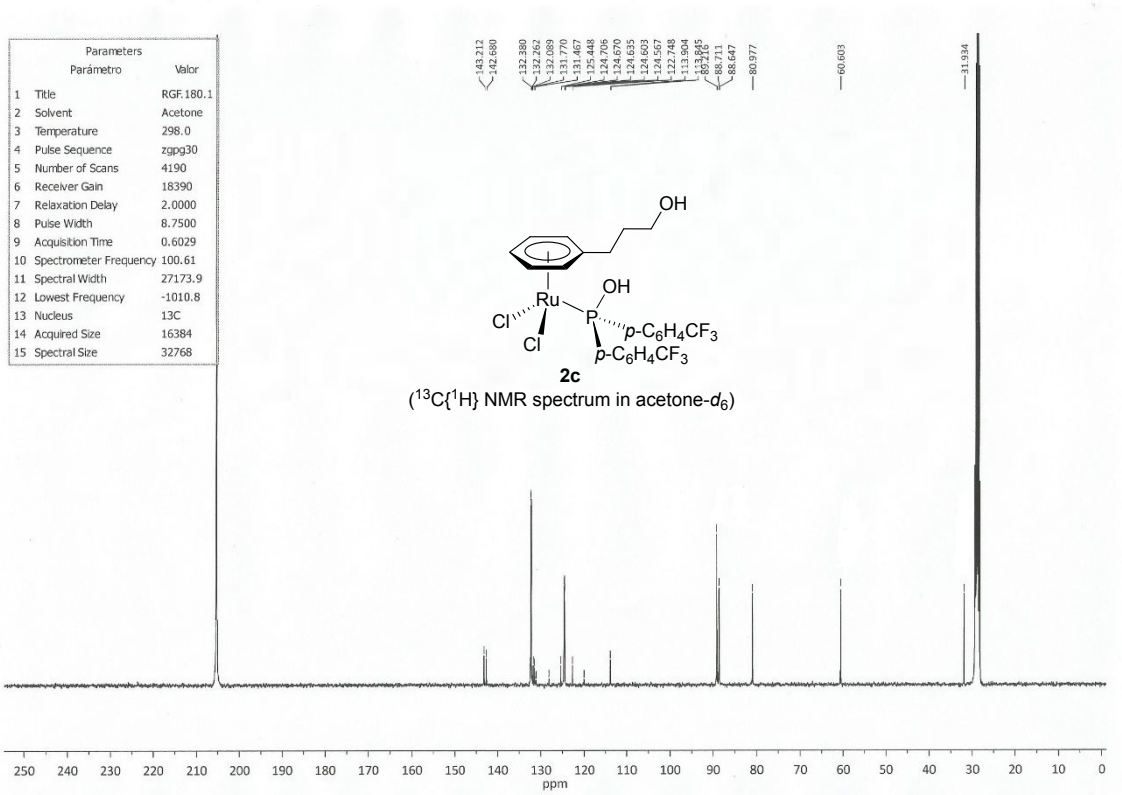

Figure S10: ^{13}C{^{1}H} NMR spectrum (100 MHz, acetone-d_6) of complex **2c**.

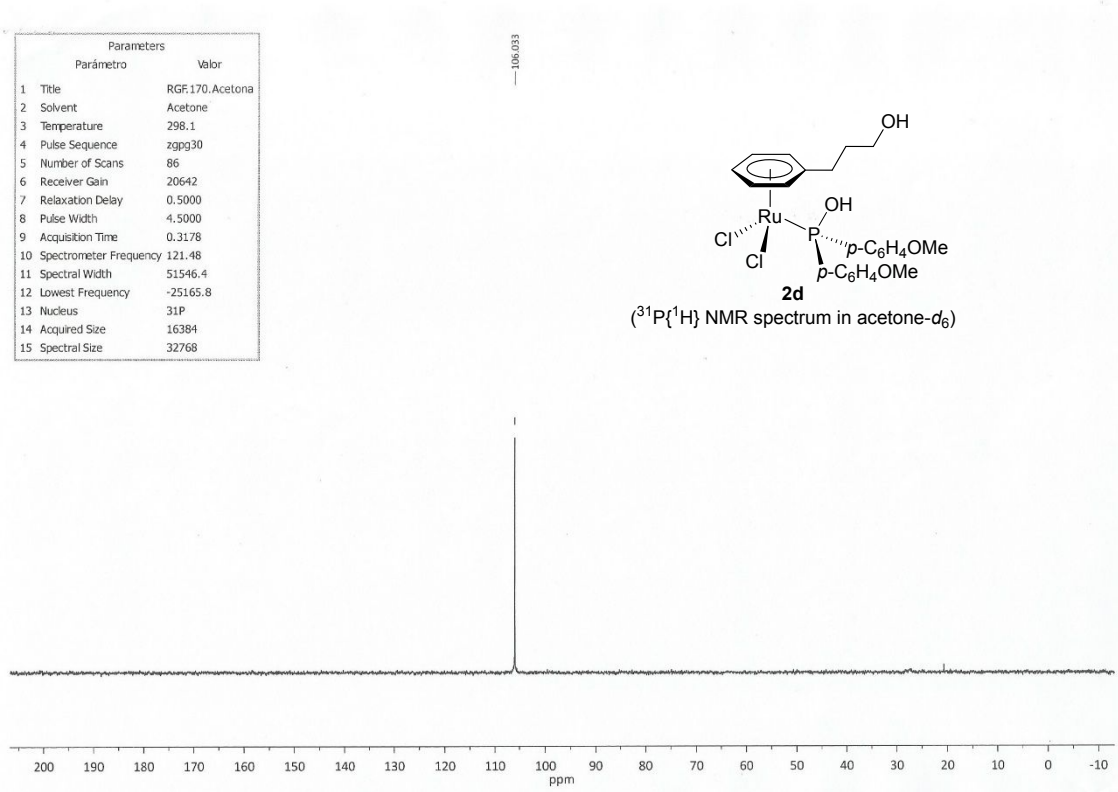

Figure S11: $^{31}P\{^{1}H\}$ NMR spectrum (121 MHz, acetone-d_6) of complex **2d**.

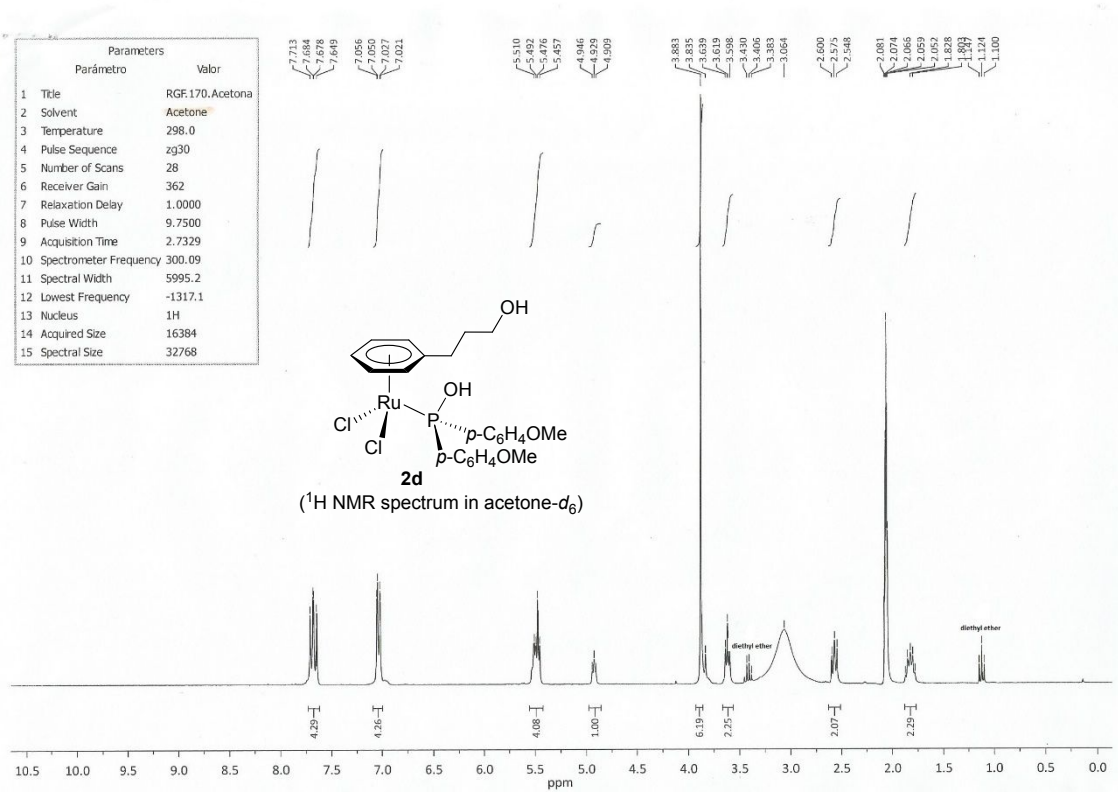

Figure S12: ^{1}H NMR spectrum (300 MHz, acetone-d_6) of complex **2d**.

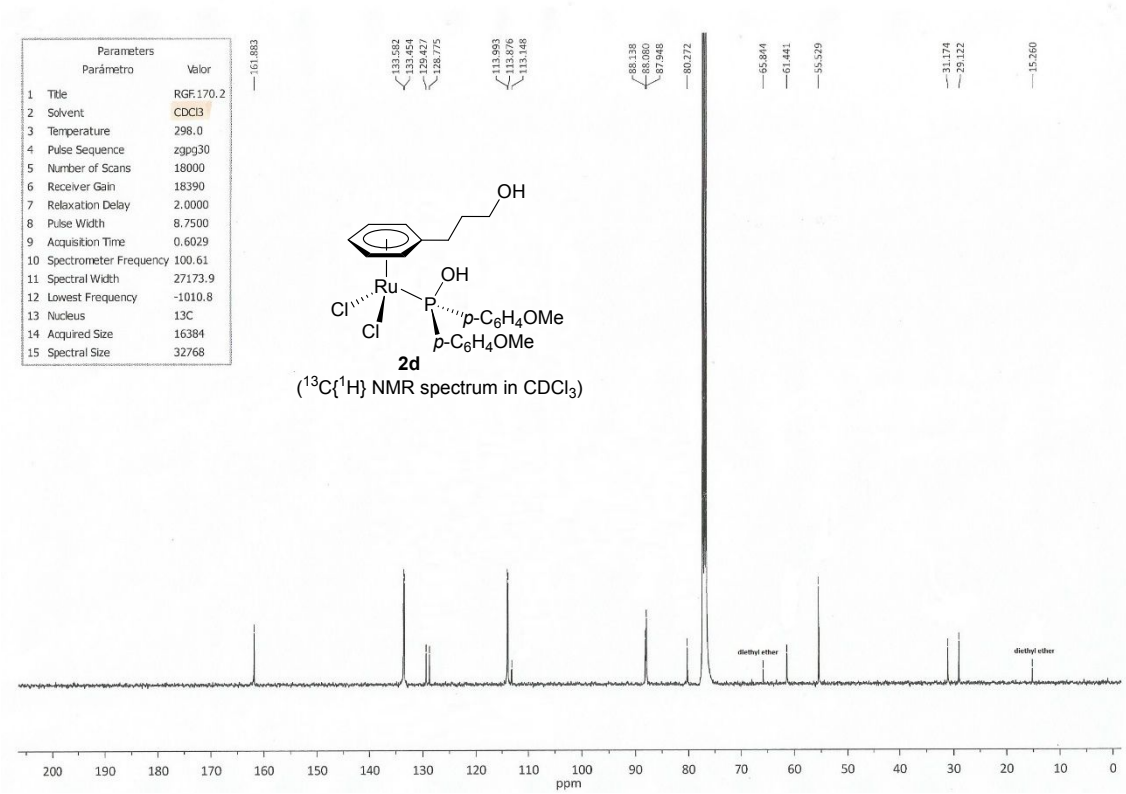

Figure S13: $^{13}C\{^1H\}$ NMR spectrum (100 MHz, $CDCl_3$) of complex **2d**.

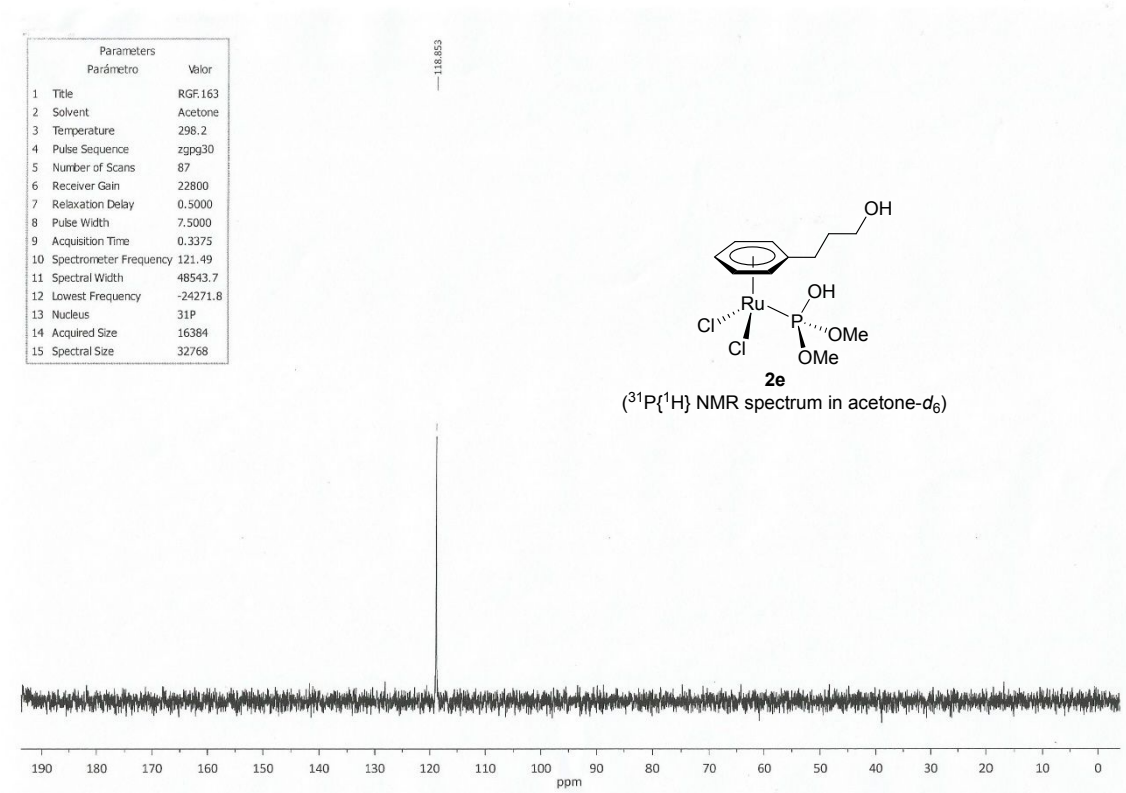

Figure S14: $^{31}P\{^1H\}$ NMR spectrum (121 MHz, acetone-d_6) of complex **2e**.

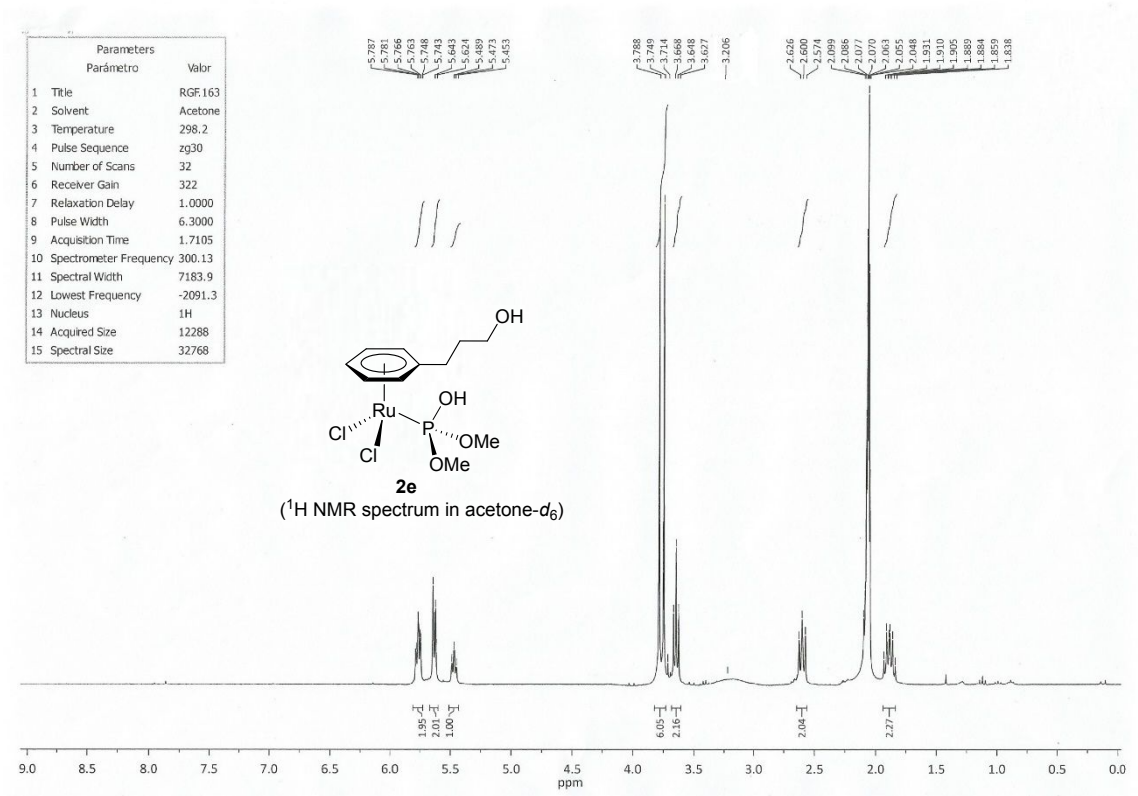

Figure S15: ^{1}H NMR spectrum (300 MHz, acetone-d_6) of complex **2e**.

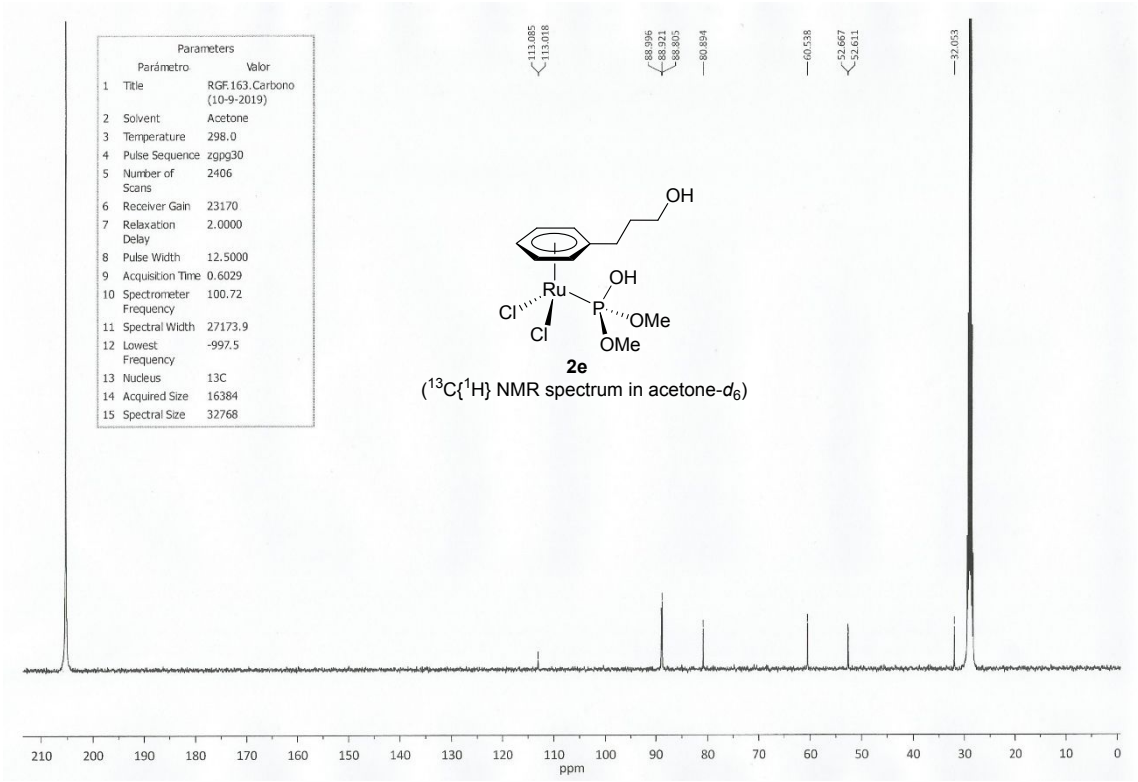

Figure S16: ^{13}C{^{1}H} NMR spectrum (100 MHz, acetone-d_6) of complex **2e**.

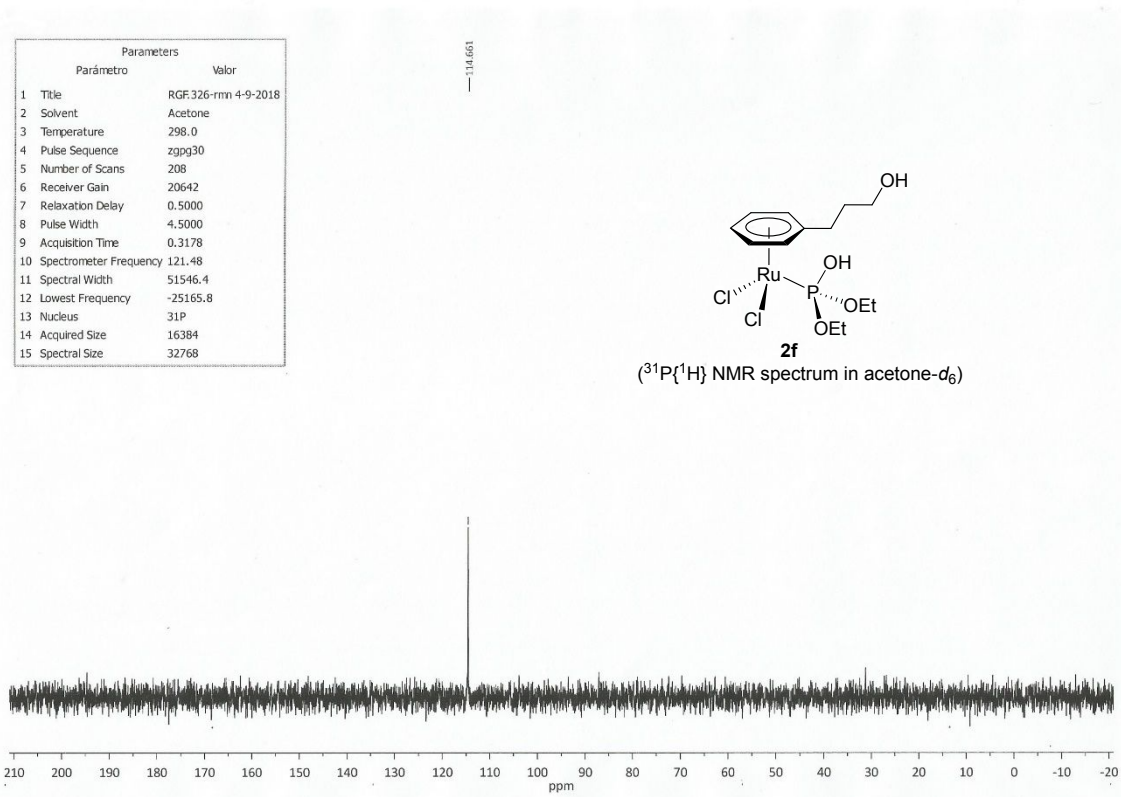

Figure S17: $^{31}P\{^{1}H\}$ NMR spectrum (121 MHz, acetone-d_6) of complex **2f**.

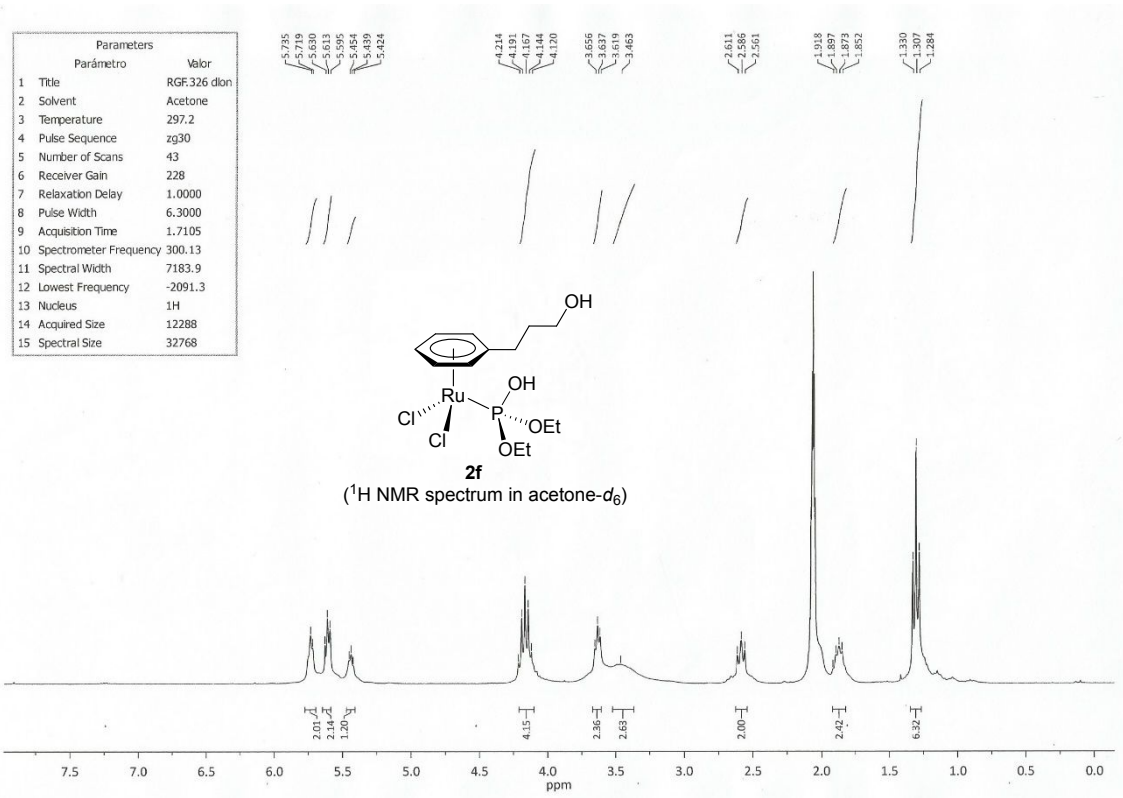

Figure S18: ^{1}H NMR spectrum (300 MHz, acetone-d_6) of complex **2f**.

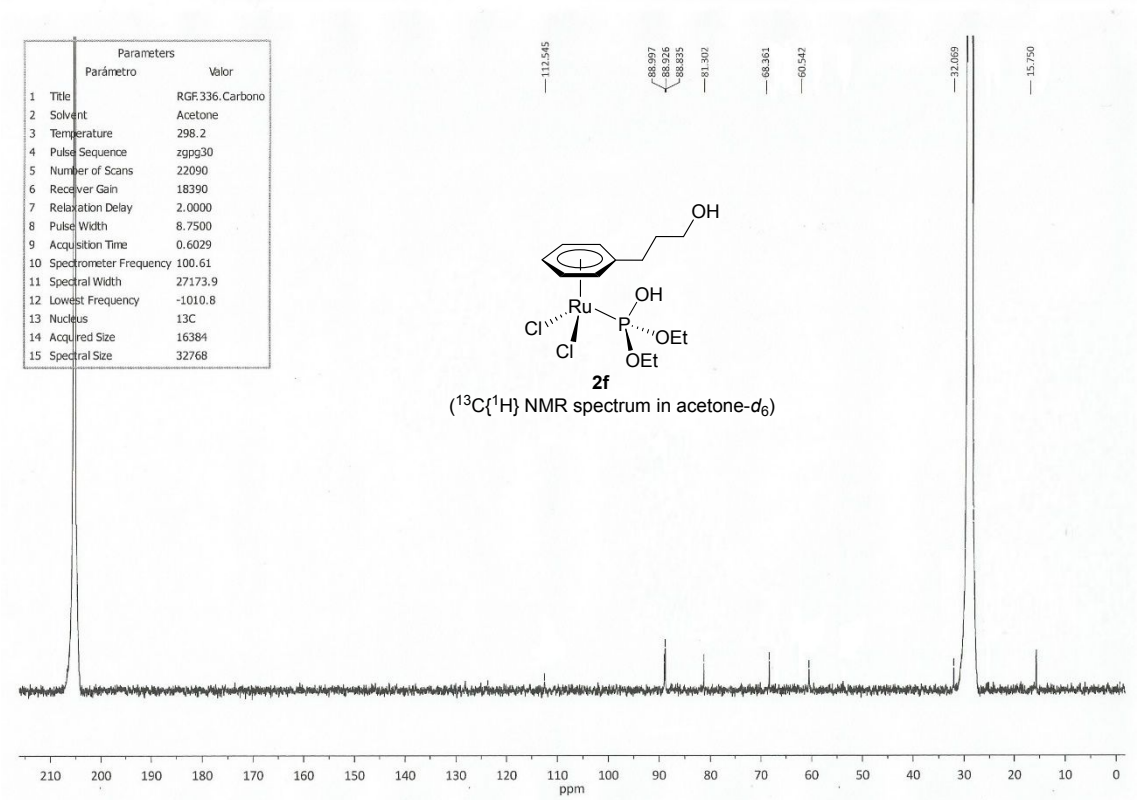

Figure S19: $^{13}C\{^{1}H\}$ NMR spectrum (100 MHz, acetone-d_6) of complex **2f**.

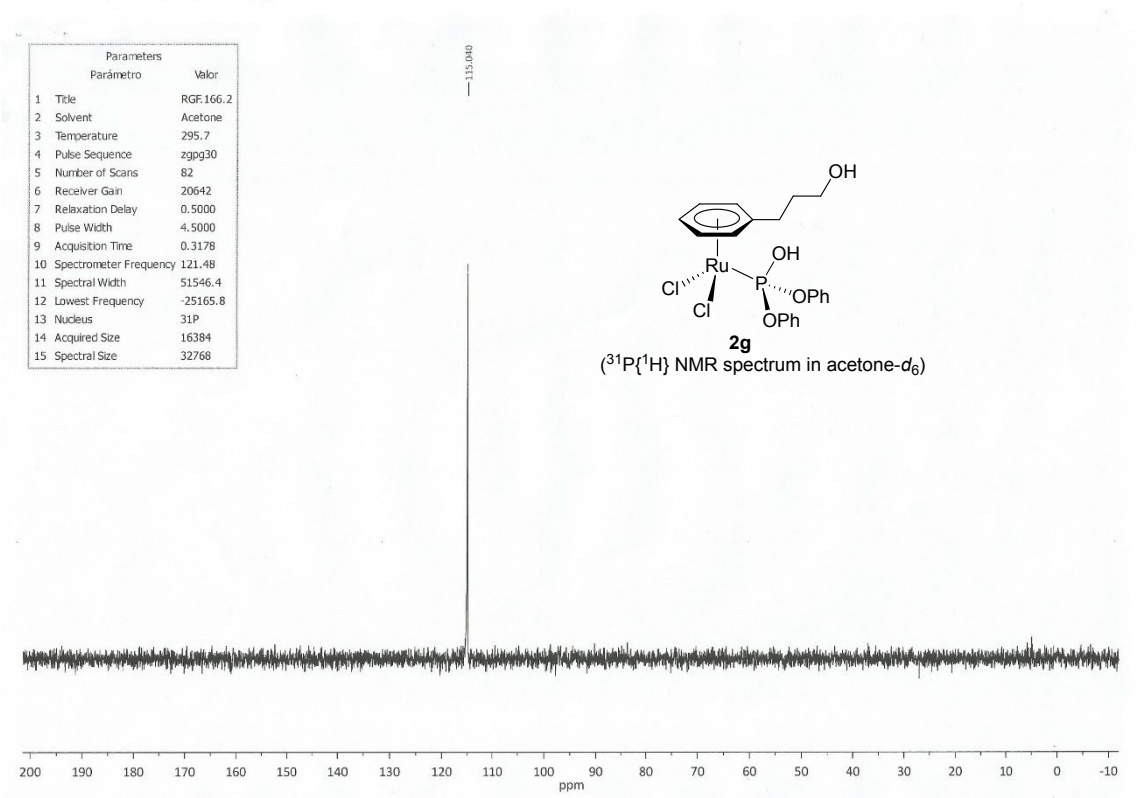

Figure S20: $^{31}P\{^{1}H\}$ NMR spectrum (121 MHz, acetone-d_6) of complex **2g**.

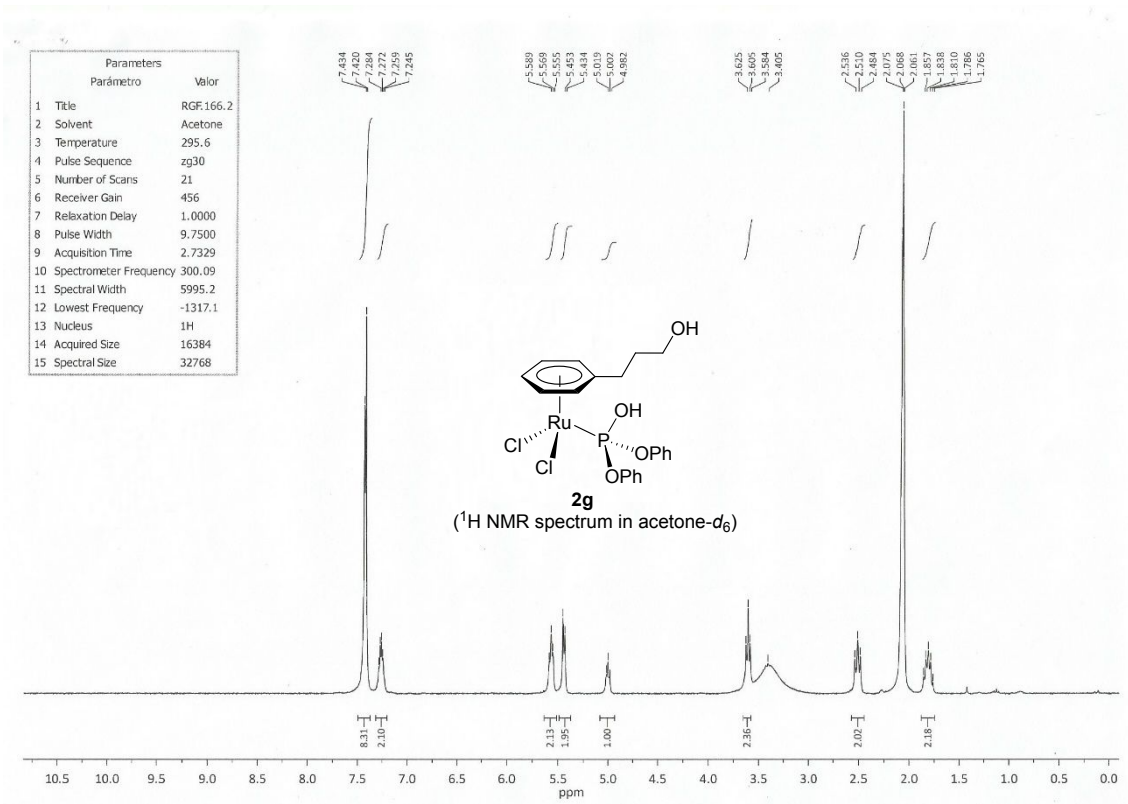

Figure S21: ^{1}H NMR spectrum (300 MHz, acetone-d_6) of complex **2g**.

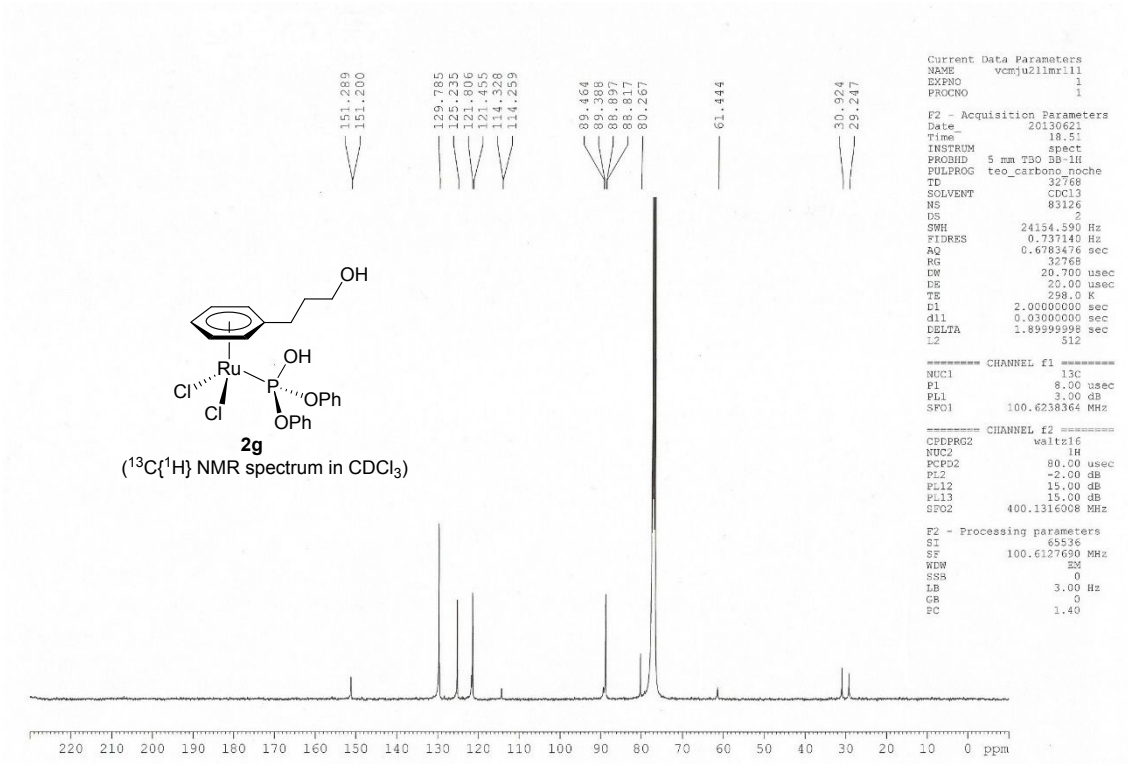

Figure S22: ^{13}C{^{1}H} NMR spectrum (100 MHz, $CDCl_3$) of complex **2g**.

NMR spectra of the isolated (1-propenyl)benzene derivatives 4a-k

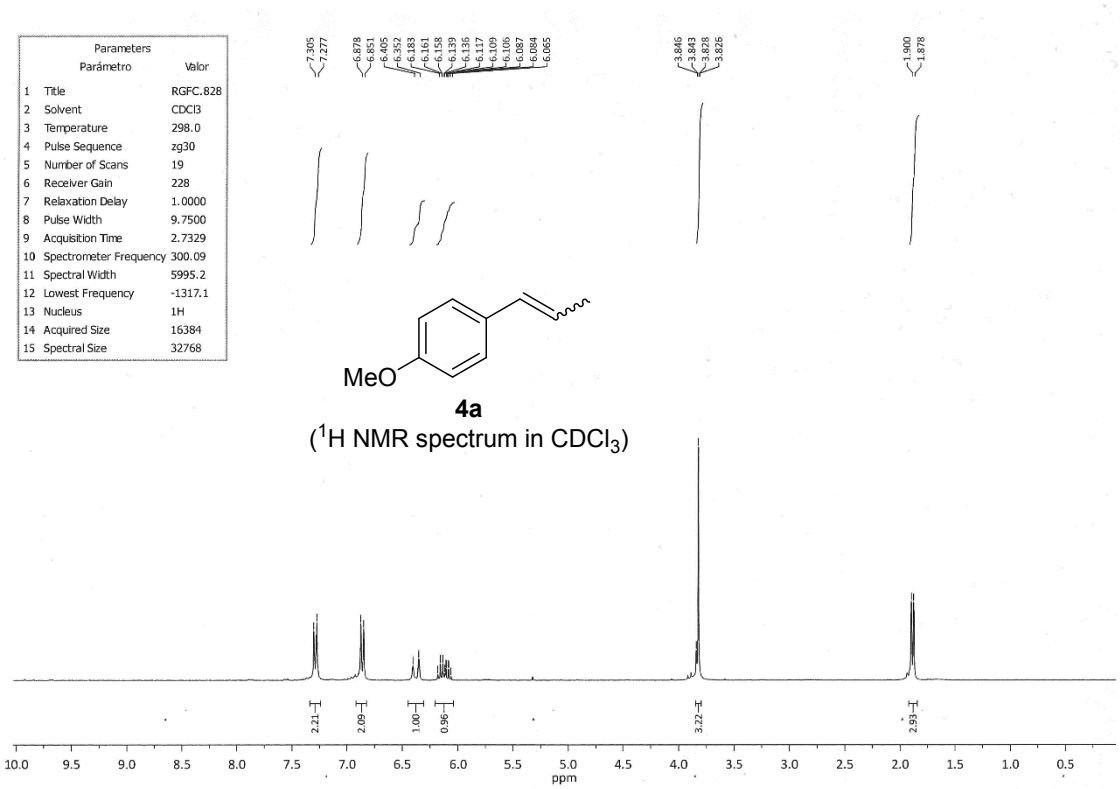

Figure S23: ^{1}H NMR spectrum (300 MHz, $CDCl_3$) of **4a**.

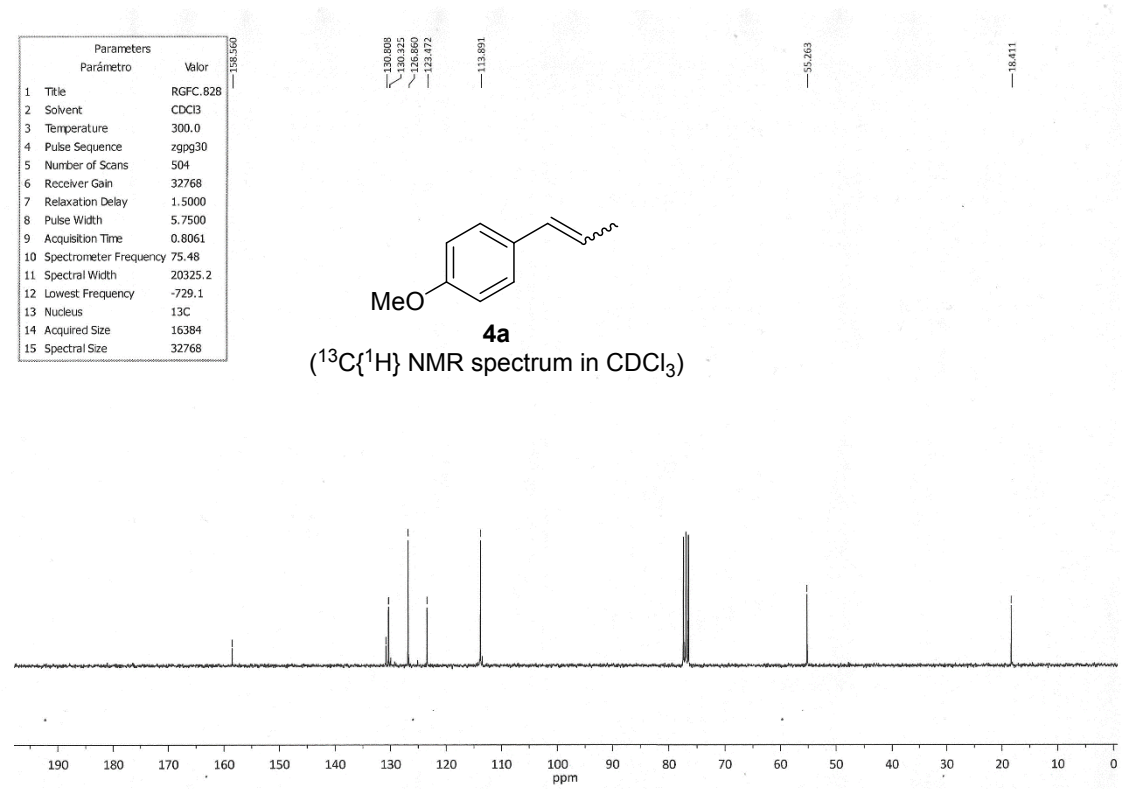

Figure S24: ^{13}C{^{1}H} NMR spectrum (75 MHz, $CDCl_3$) of **4a**.

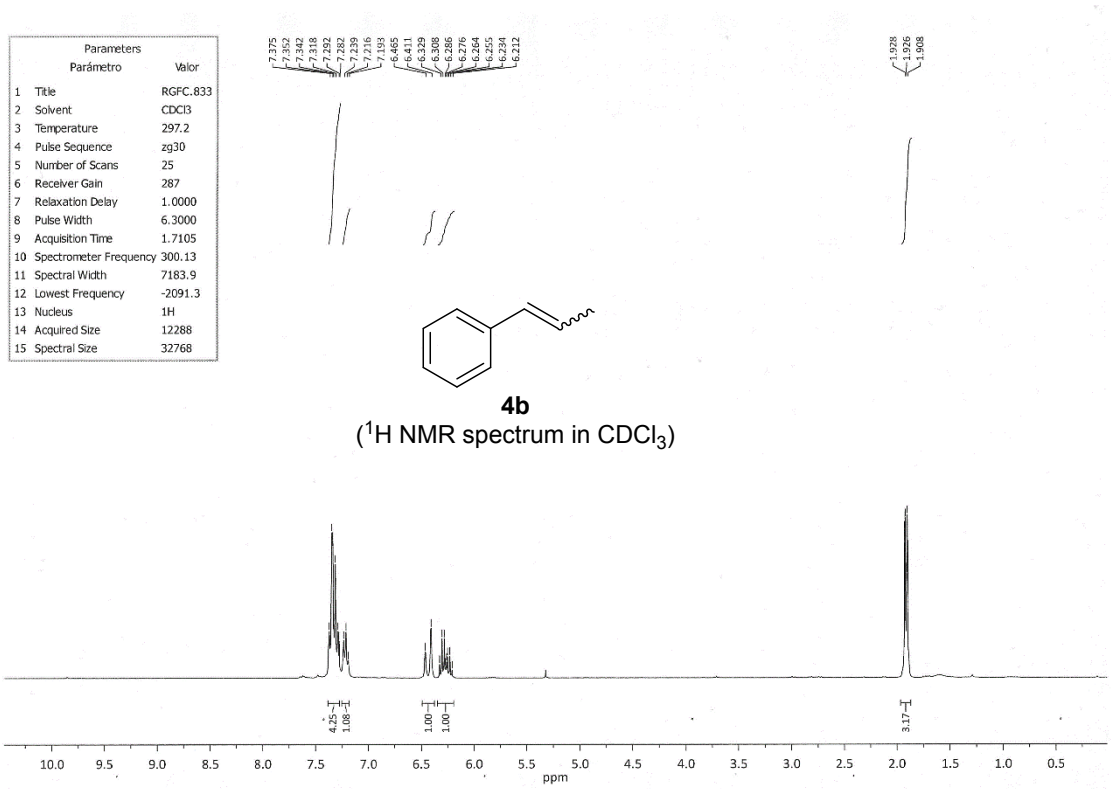

Figure S25: ^{1}H NMR spectrum (300 MHz, $CDCl_3$) of **4b**.

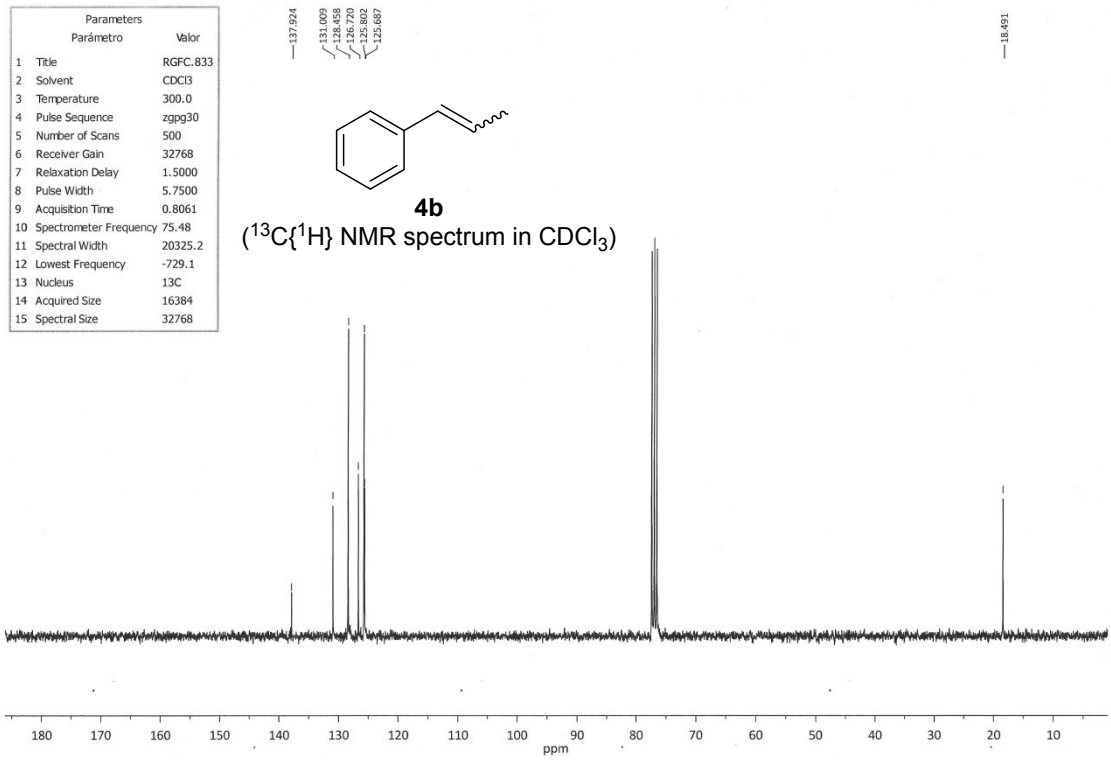

Figure S26: $^{13}C\{^{1}H\}$ NMR spectrum (75 MHz, $CDCl_3$) of **4b**.

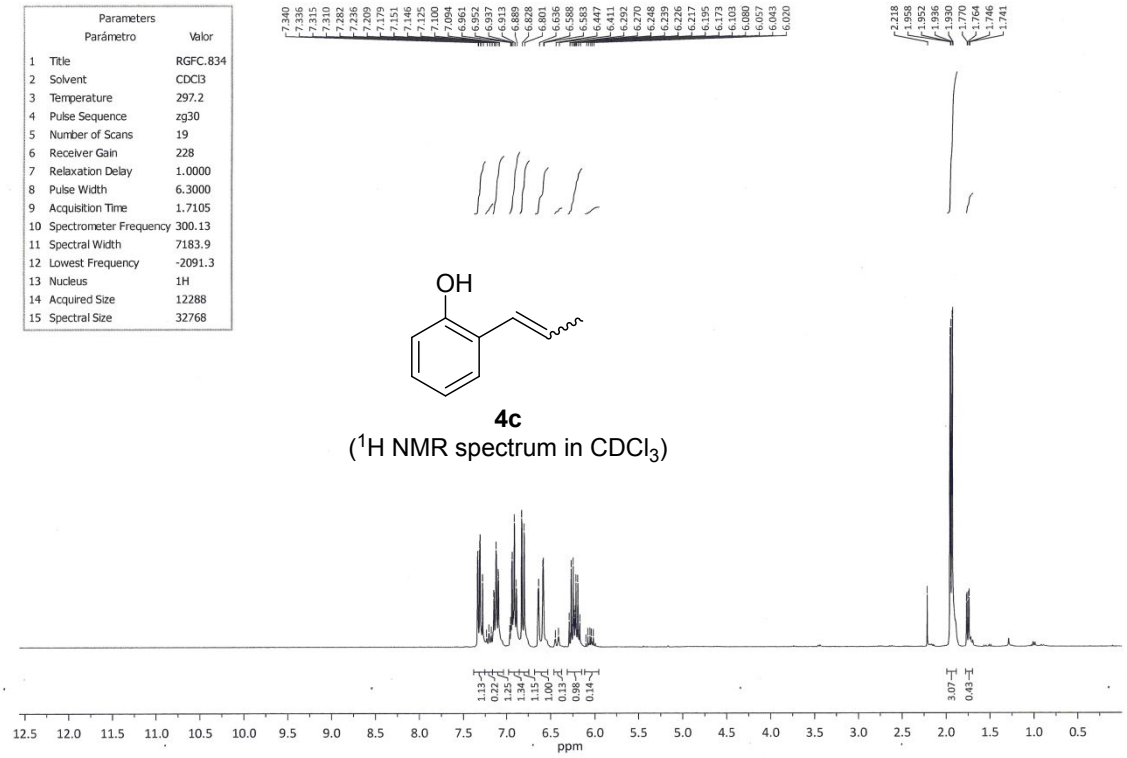

Figure S27: ^{1}H NMR spectrum (300 MHz, $CDCl_3$) of **4c**.

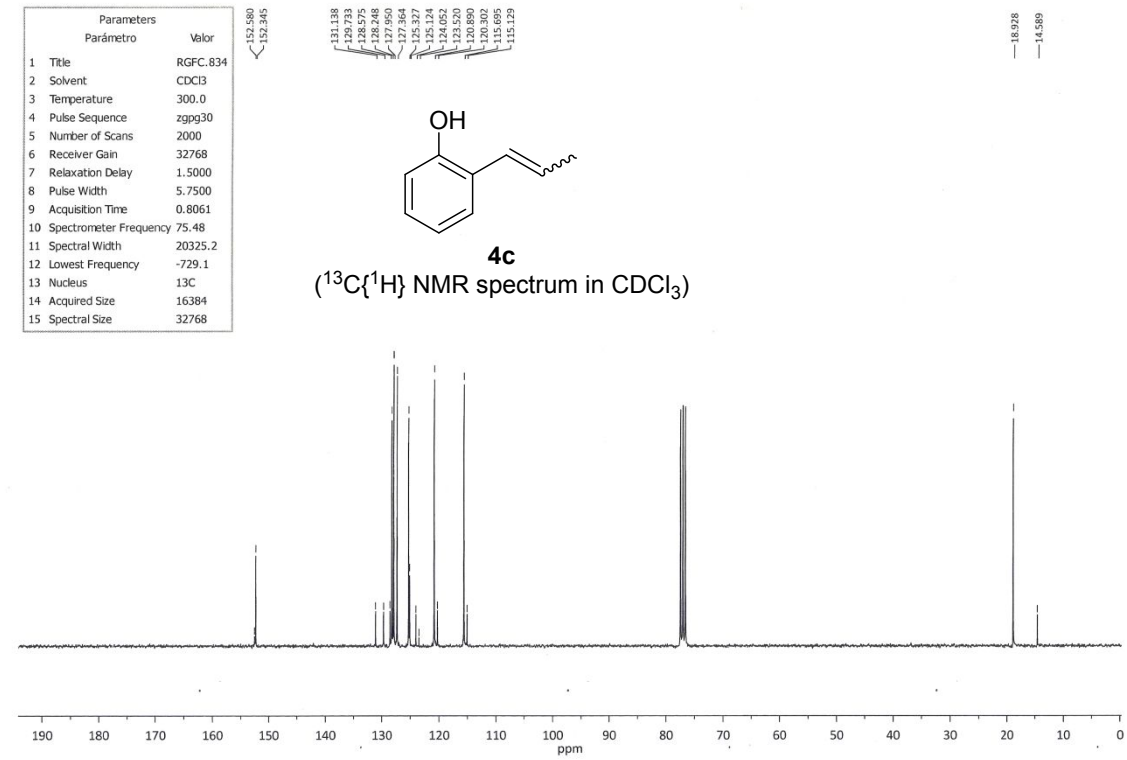

Figure S28: ^{13}C{^{1}H} NMR spectrum (75 MHz, $CDCl_3$) of **4c**.

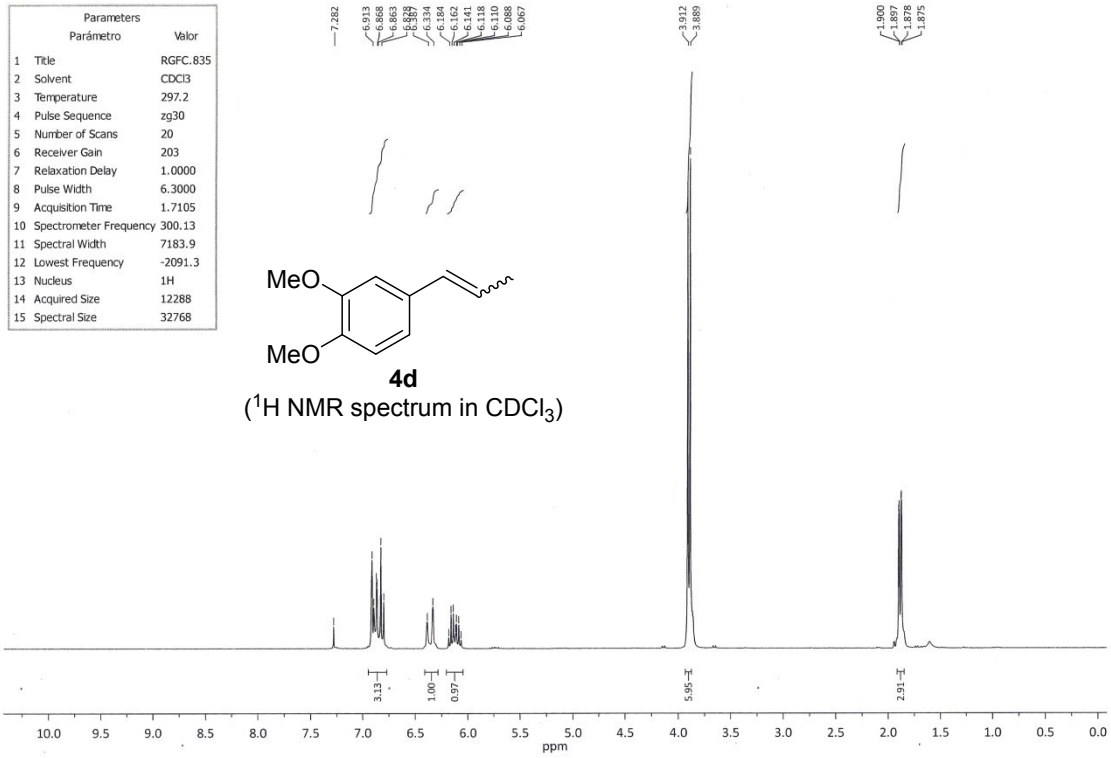

Figure S29: ^{1}H NMR spectrum (300 MHz, $CDCl_3$) of **4d**.

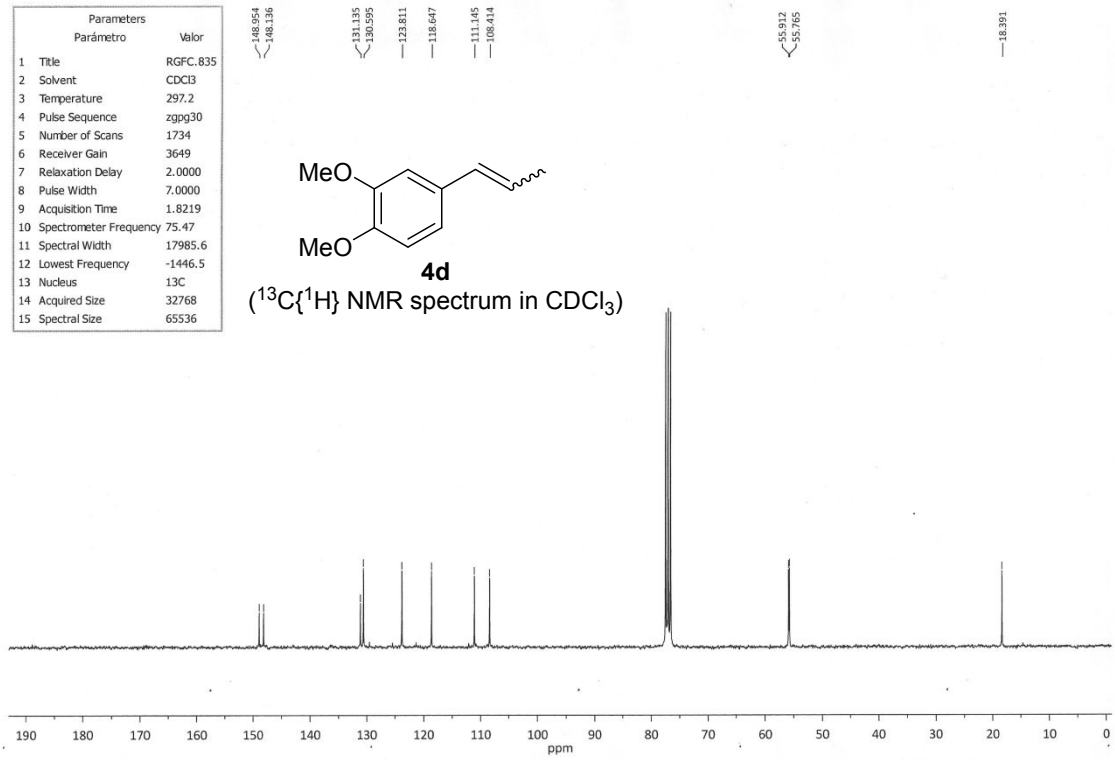

Figure S30: ^{13}C{^{1}H} NMR spectrum (75 MHz, $CDCl_3$) of **4d**.

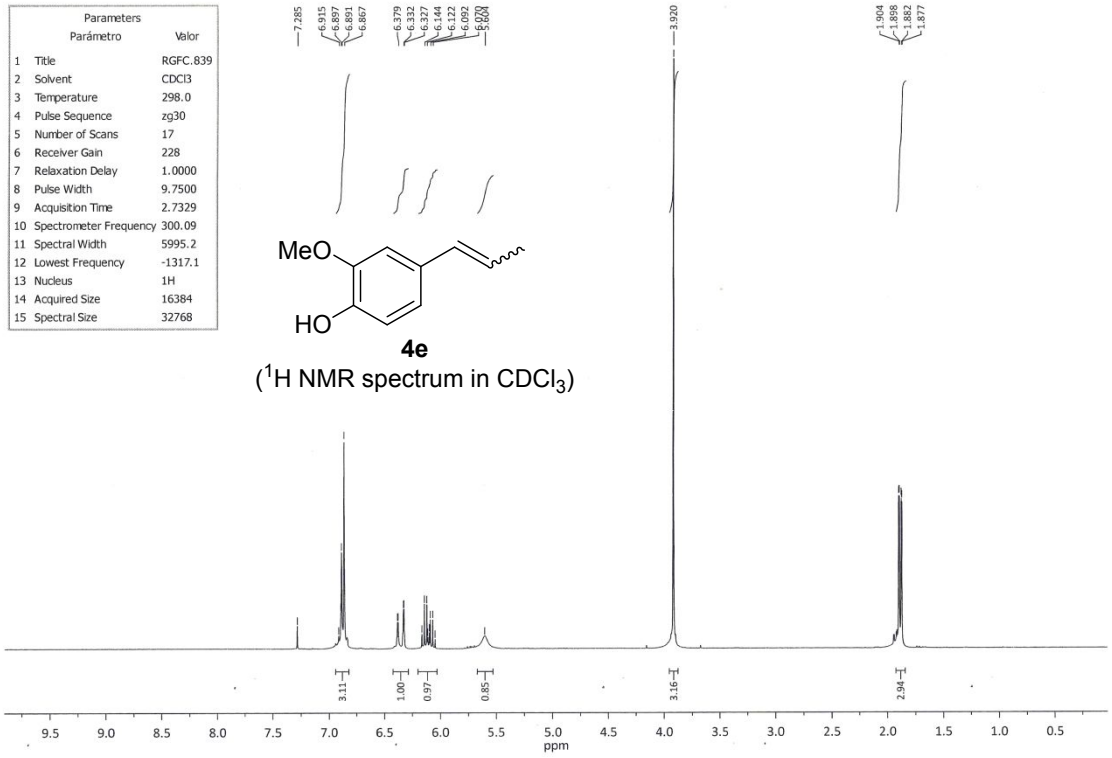

Figure S31: ^{1}H NMR spectrum (300 MHz, $CDCl_3$) of **4e**.

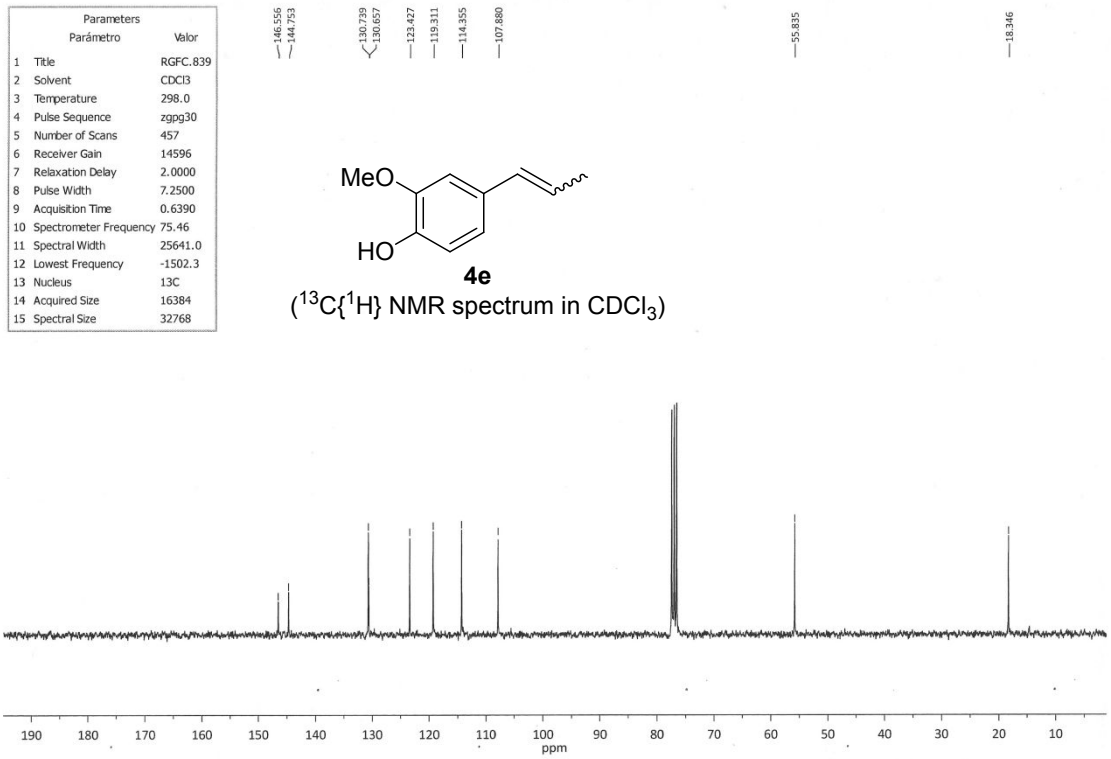

Figure S32: ^{13}C{^{1}H} NMR spectrum (75 MHz, $CDCl_3$) of **4e**.

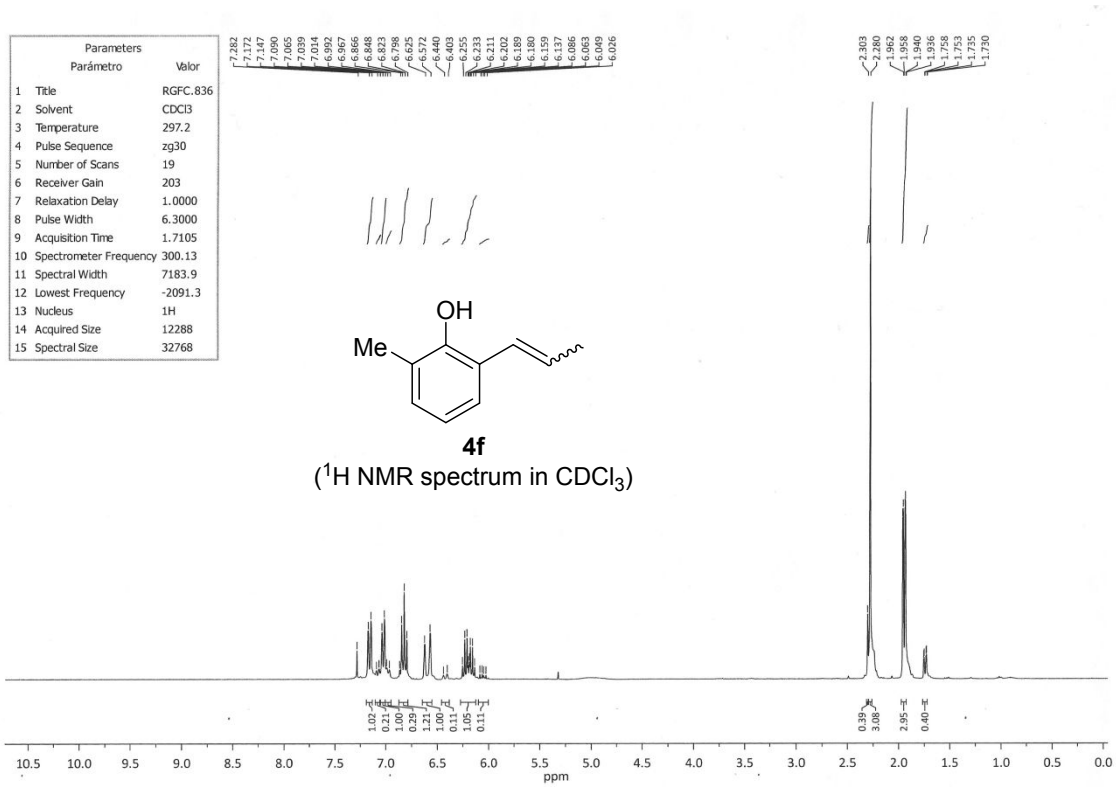

Figure S33: ^{1}H NMR spectrum (300 MHz, $CDCl_3$) of **4f**.

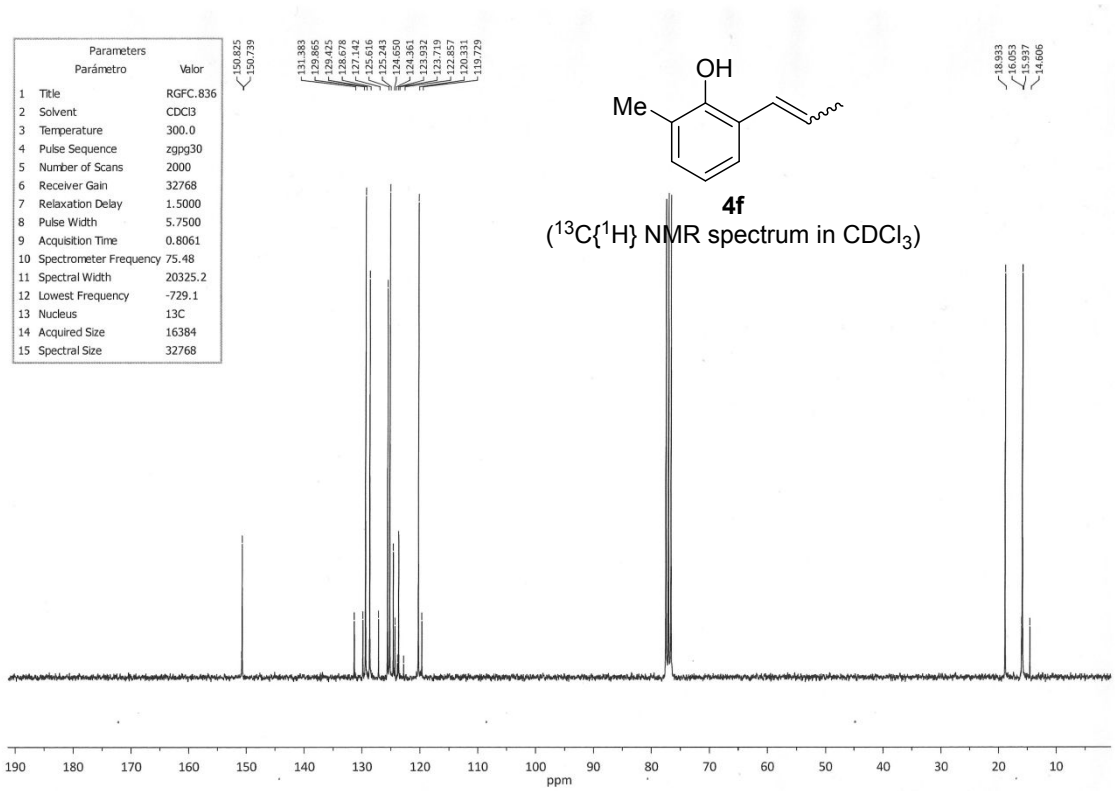

Figure S34: ^{13}C{^{1}H} NMR spectrum (75 MHz, $CDCl_3$) of **4f**.

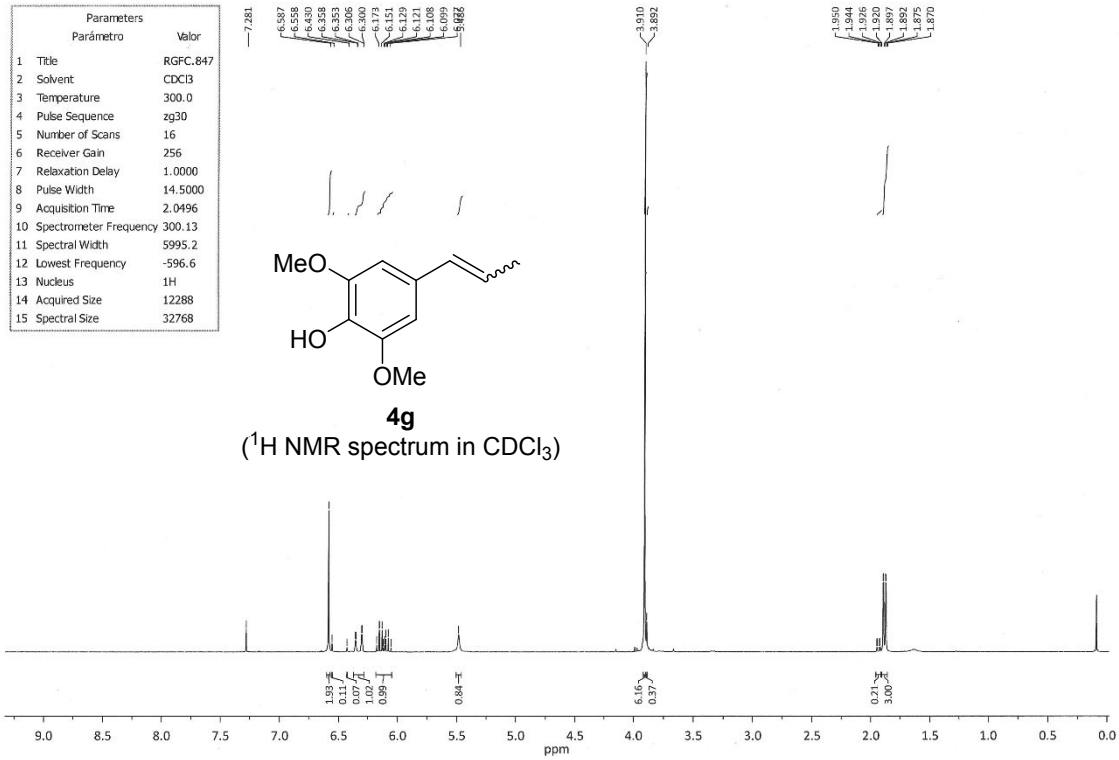

Figure S35: ^{1}H NMR spectrum (300 MHz, $CDCl_3$) of **4g**.

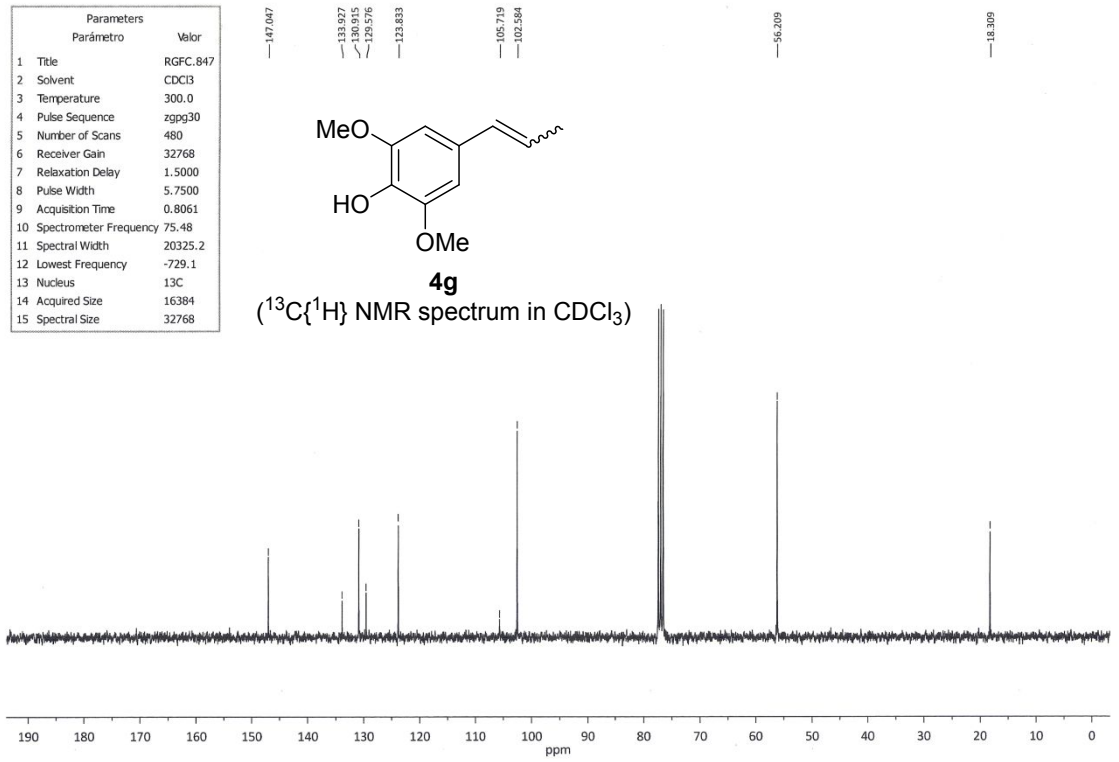

Figure S36: ^{13}C{^{1}H} NMR spectrum (75 MHz, $CDCl_3$) of **4g**.

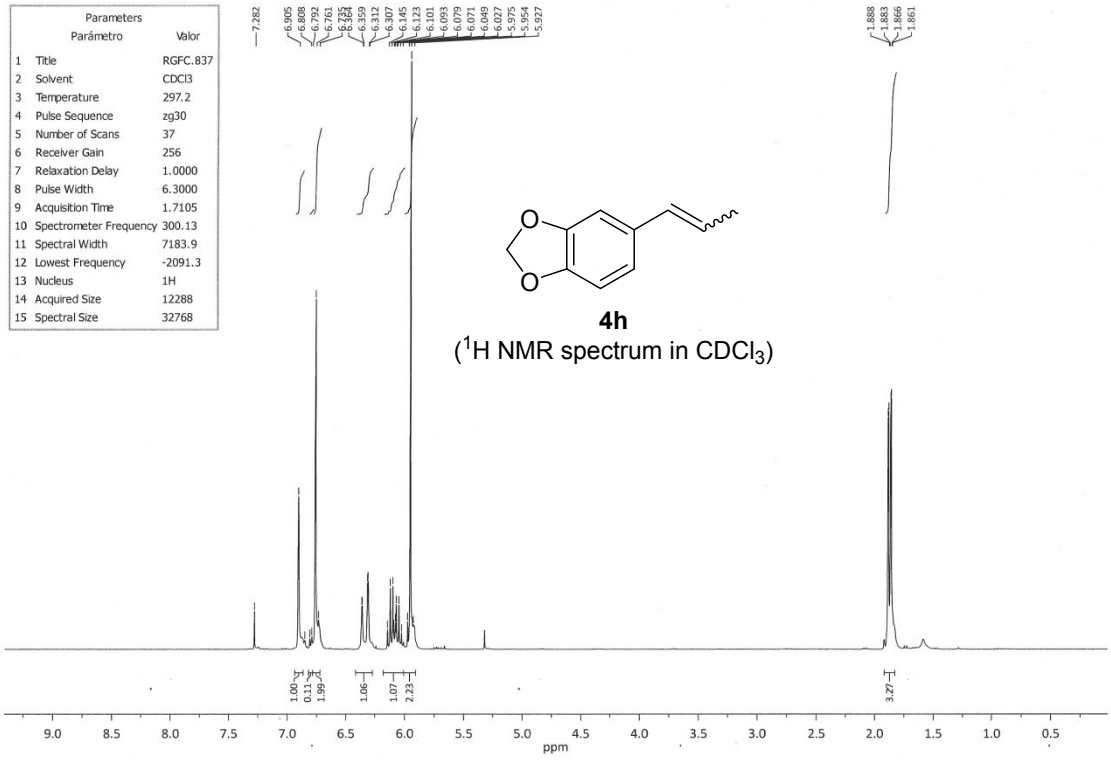

Figure S37: ^{1}H NMR spectrum (300 MHz, $CDCl_3$) of **4h**.

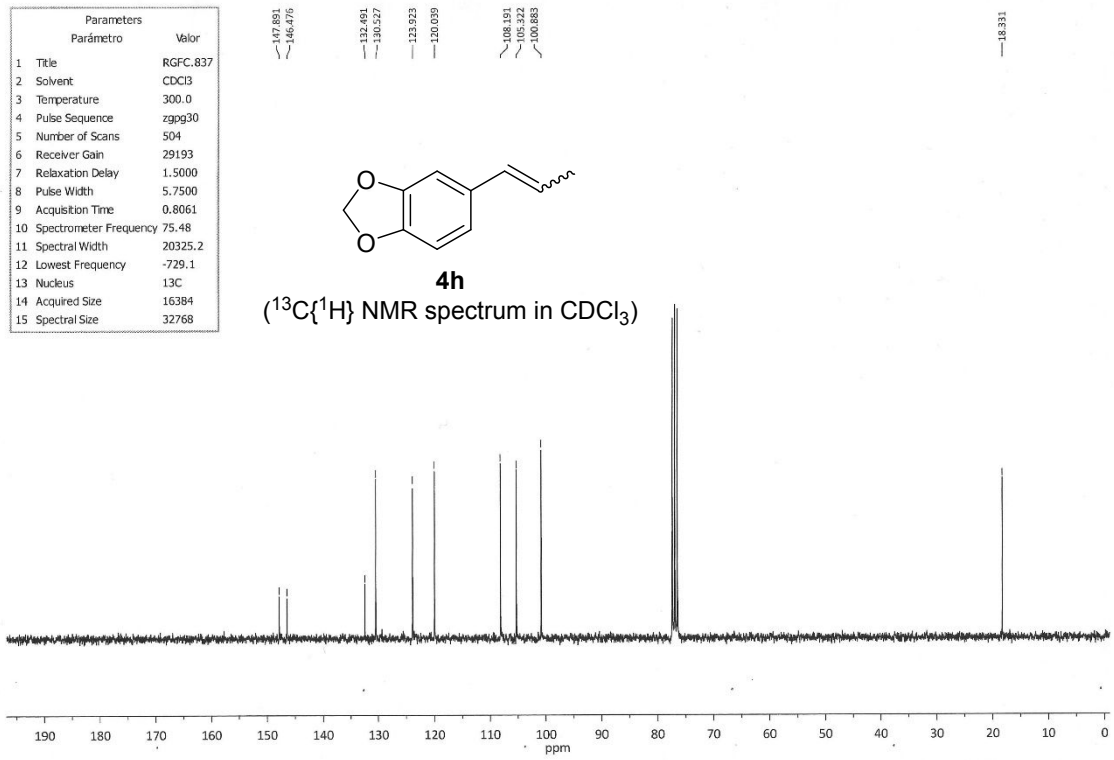

Figure S38: ^{13}C{^{1}H} NMR spectrum (75 MHz, $CDCl_3$) of **4h**.

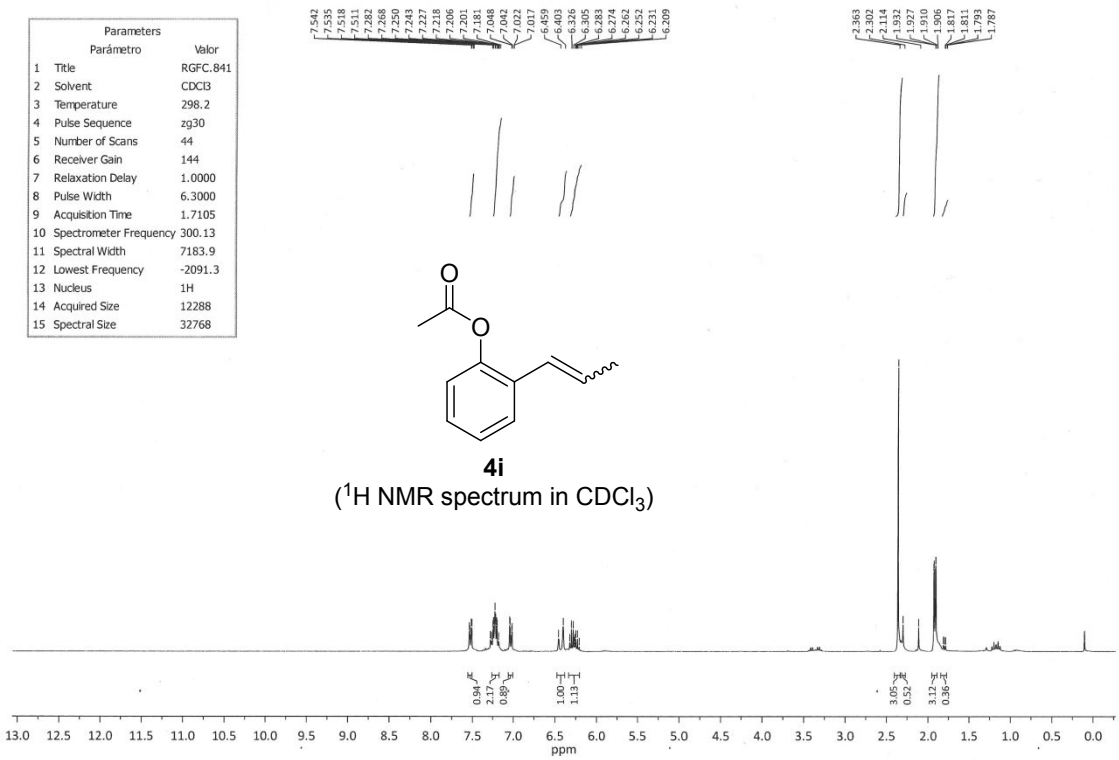

Figure S39: ^{1}H NMR spectrum (300 MHz, $CDCl_3$) of **4i**.

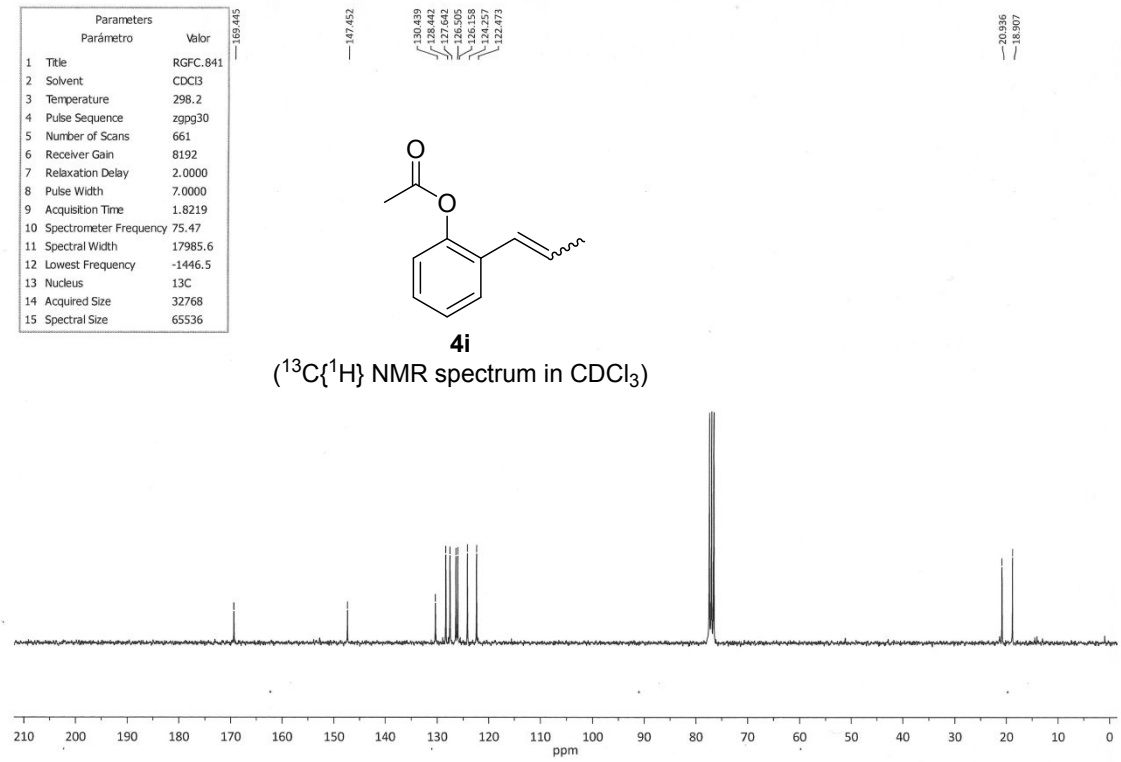

Figure S40: ^{13}C{^{1}H} NMR spectrum (75 MHz, $CDCl_3$) of **4i**.

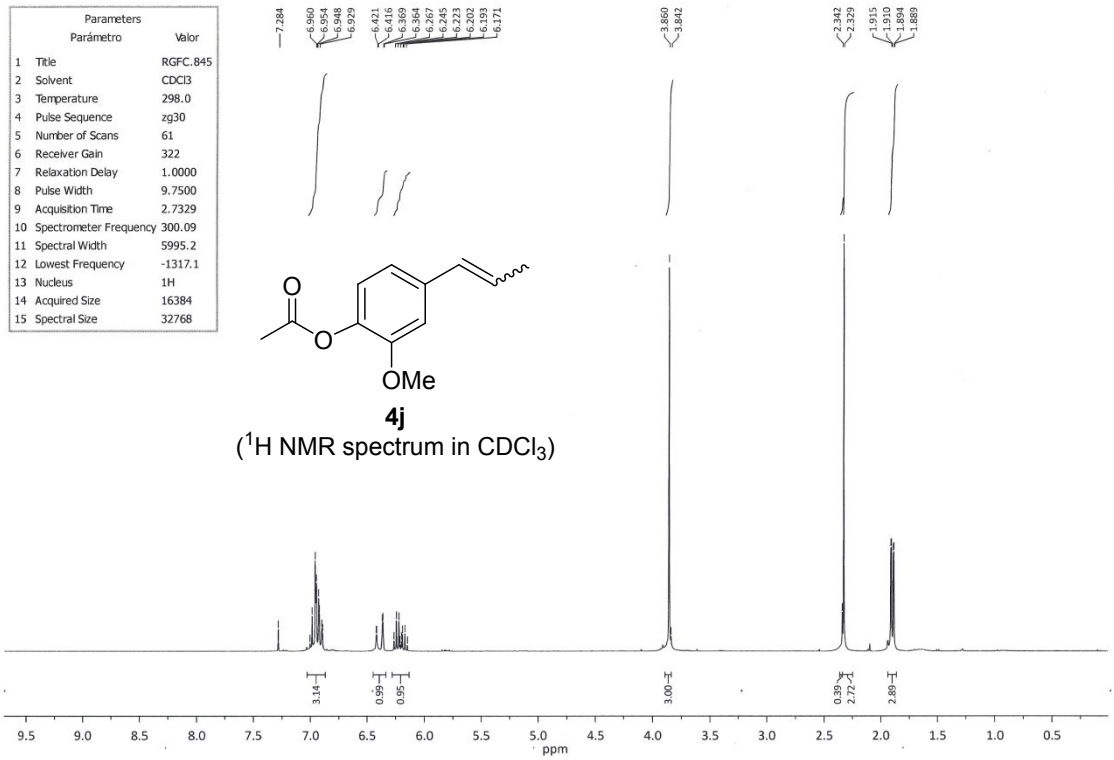

Figure S41: ^{1}H NMR spectrum (300 MHz, $CDCl_3$) of **4j**.

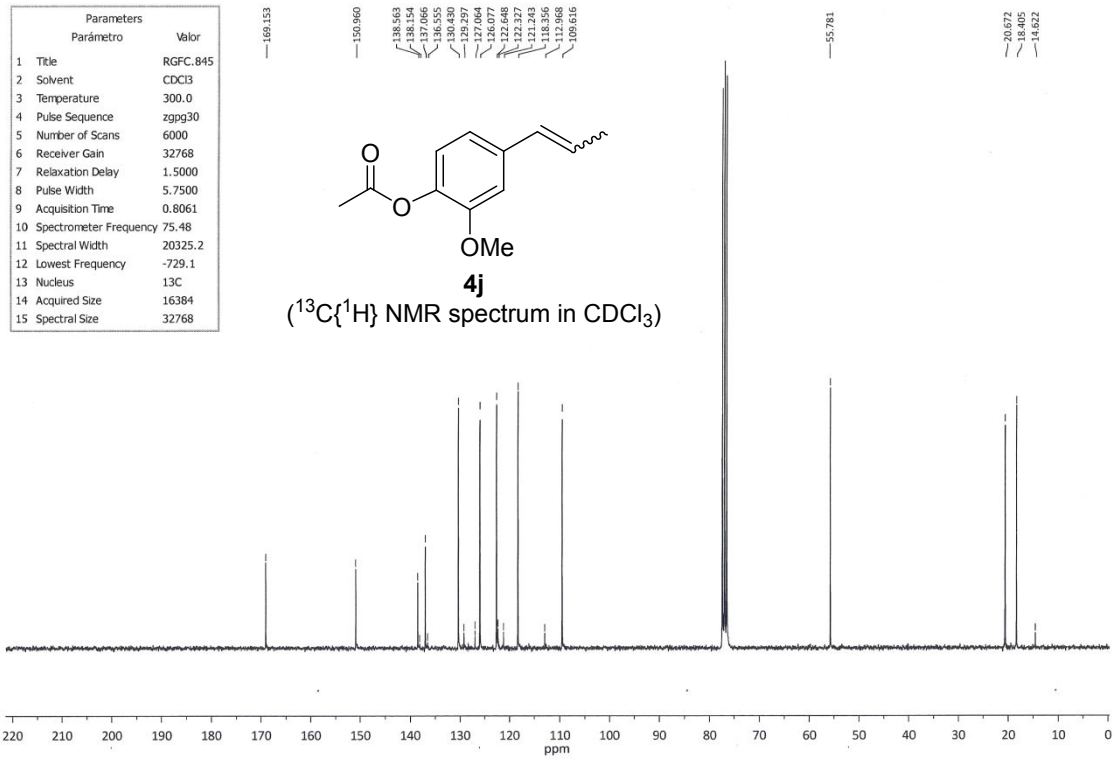

Figure S42: ^{13}C{^{1}H} NMR spectrum (75 MHz, $CDCl_3$) of **4j**.

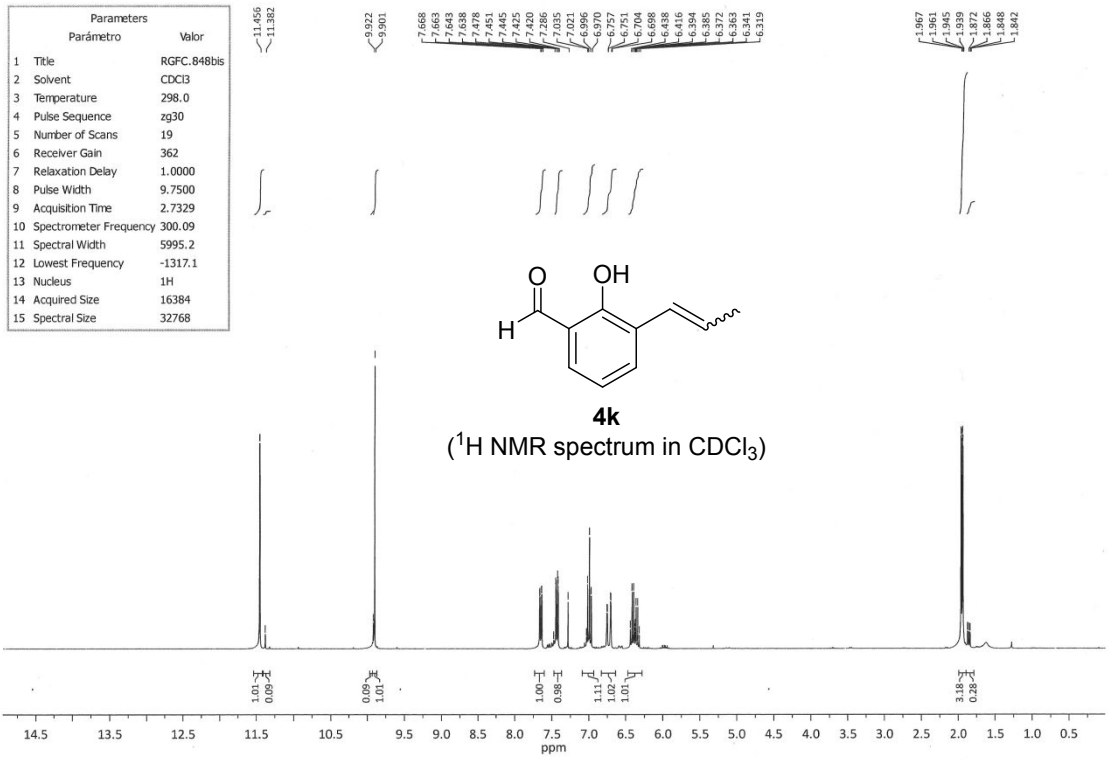

Figure S43: ^{1}H NMR spectrum (300 MHz, $CDCl_3$) of **4k**.

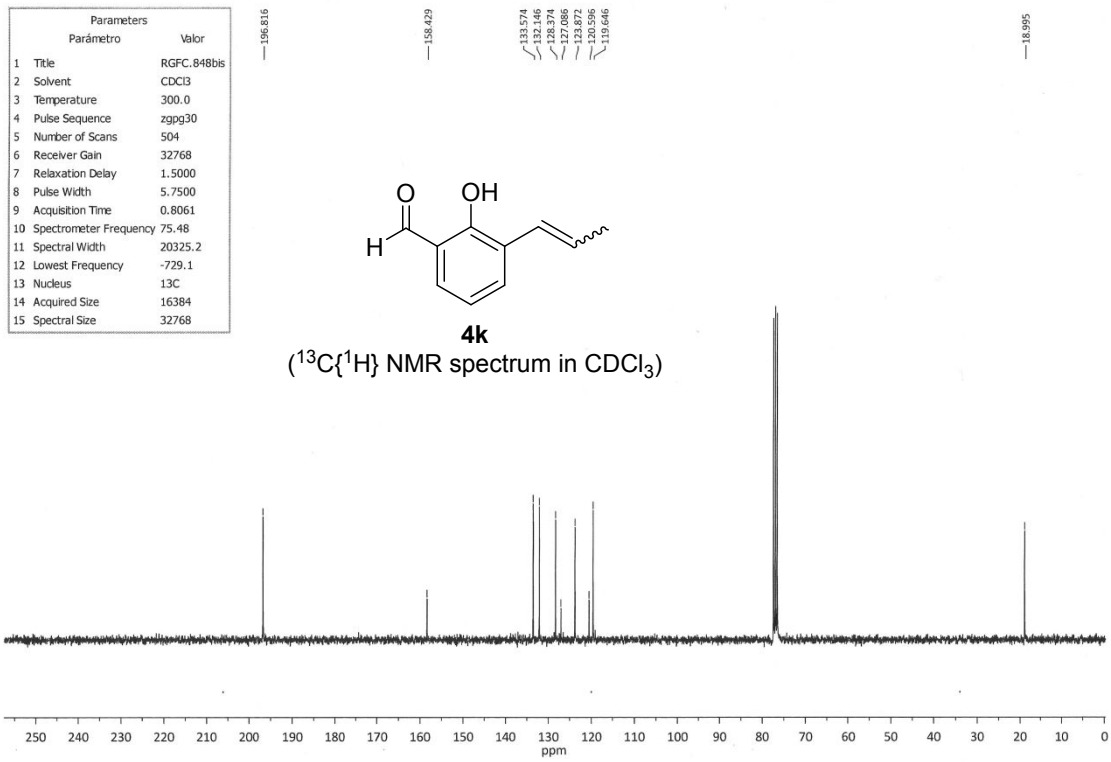

Figure S44: ^{13}C{^{1}H} NMR spectrum (75 MHz, $CDCl_3$) of **4k**.

^{1}H NMR spectra of the arylation reactions collected in Table 7

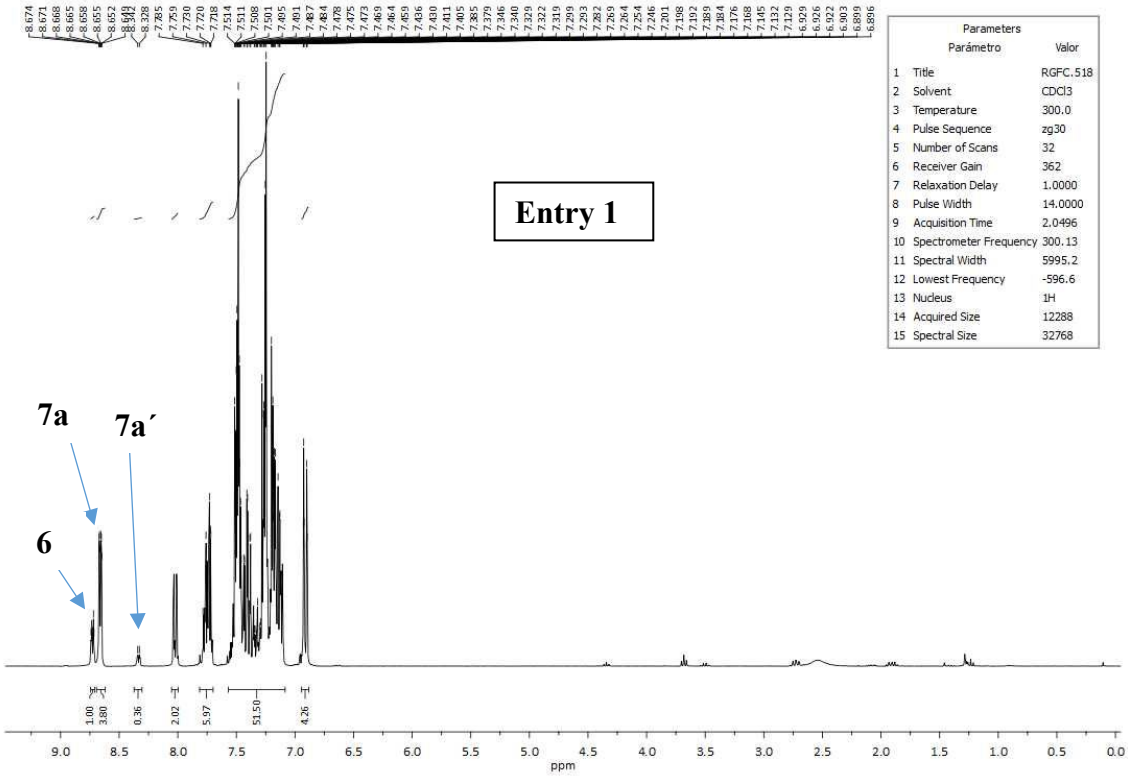

Figure S45: ^{1}H NMR spectrum (300 MHz, $CDCl_3$) of reaction collected in entry 1 of Table 7.

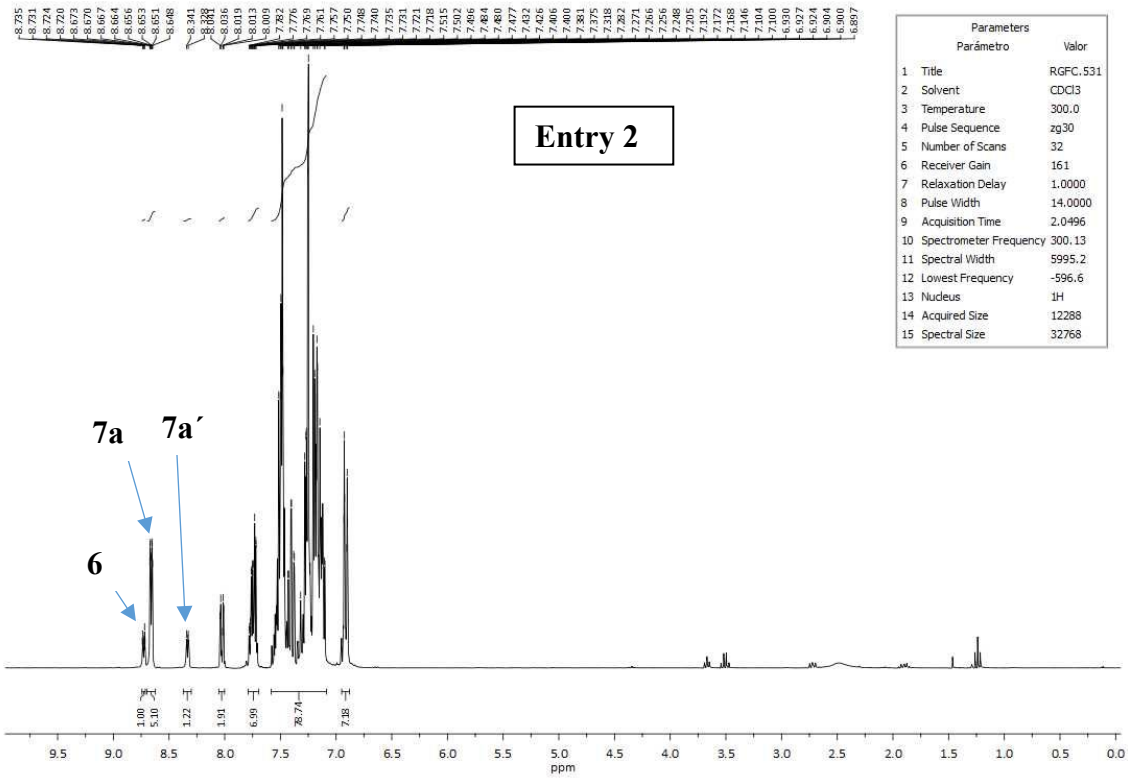

Figure S46: ^{1}H NMR spectrum (300 MHz, $CDCl_3$) of reaction collected in entry 2 of Table 7.

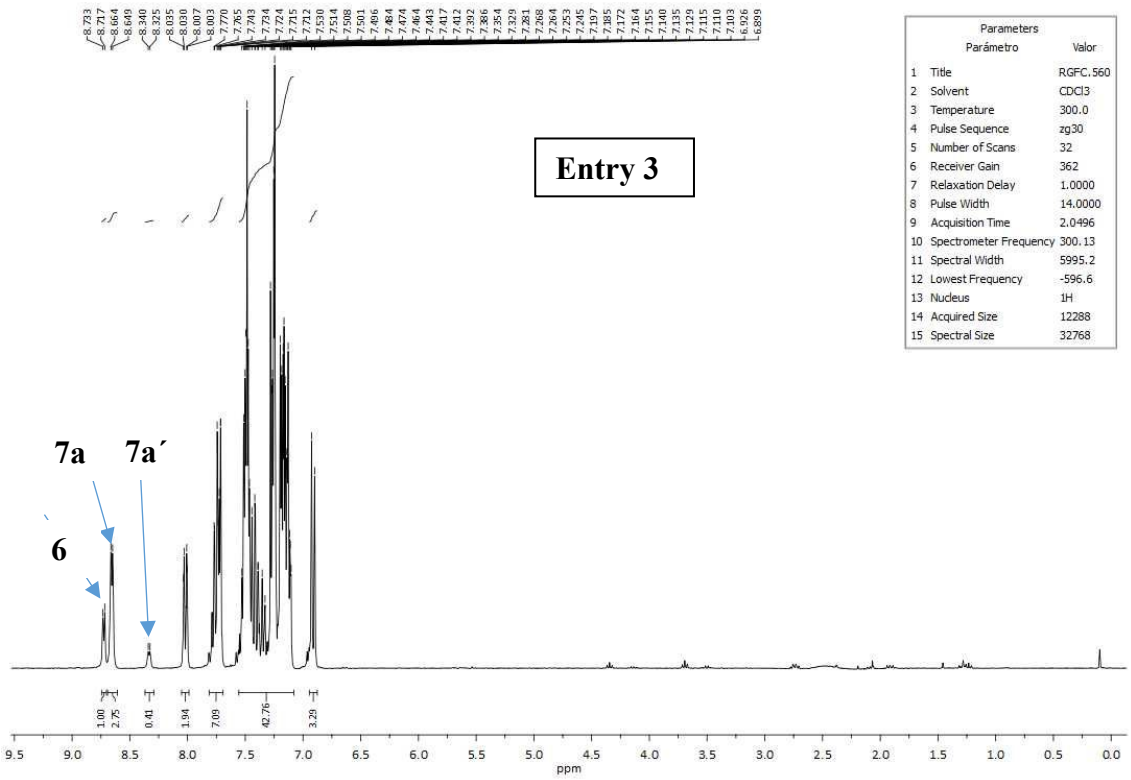

Figure S47: ^{1}H NMR spectrum (300 MHz, $CDCl_3$) of reaction collected in entry 3 of Table 7.

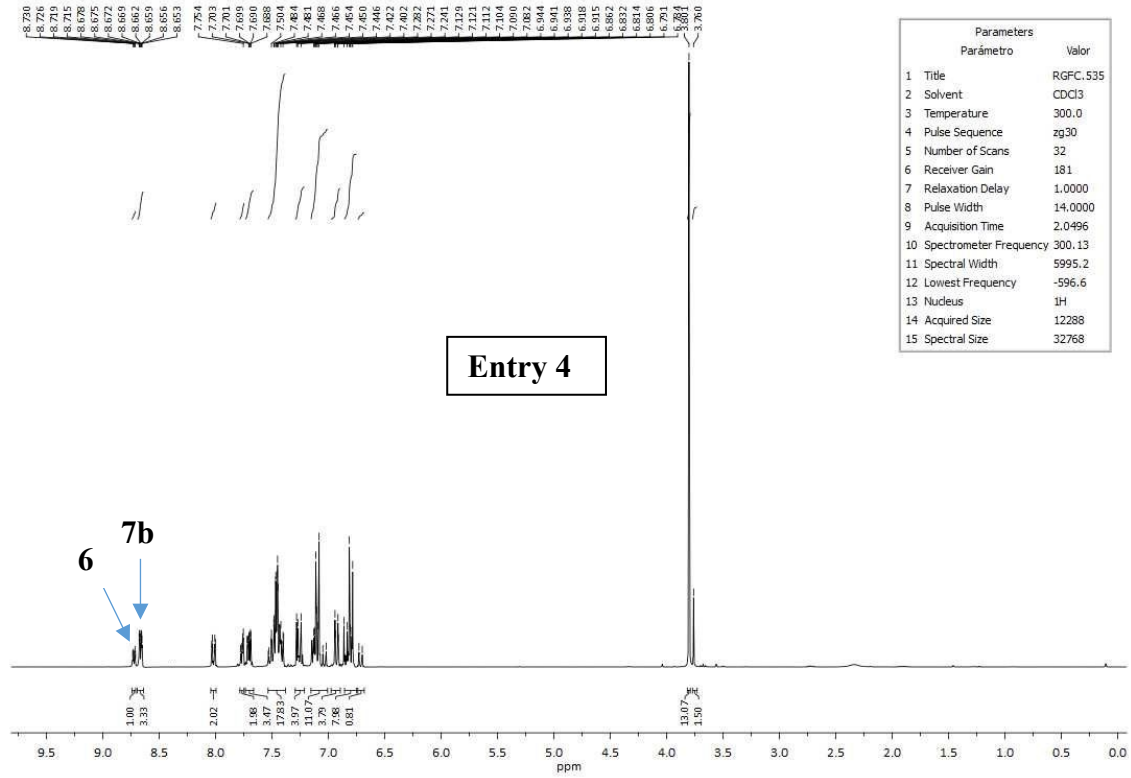

Figure S48: ^{1}H NMR spectrum (300 MHz, $CDCl_3$) of reaction collected in entry 4 of Table 7.

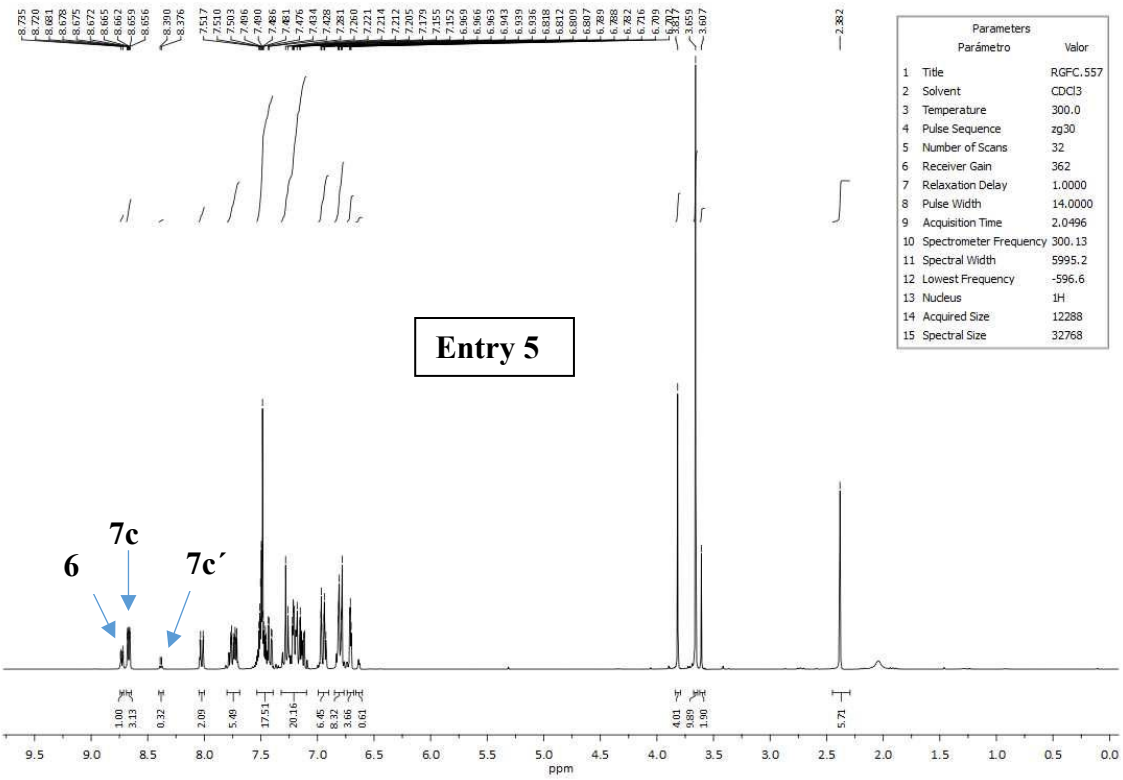

Figure S49: ^{1}H NMR spectrum (300 MHz, $CDCl_3$) of reaction collected in entry 5 of Table 7.

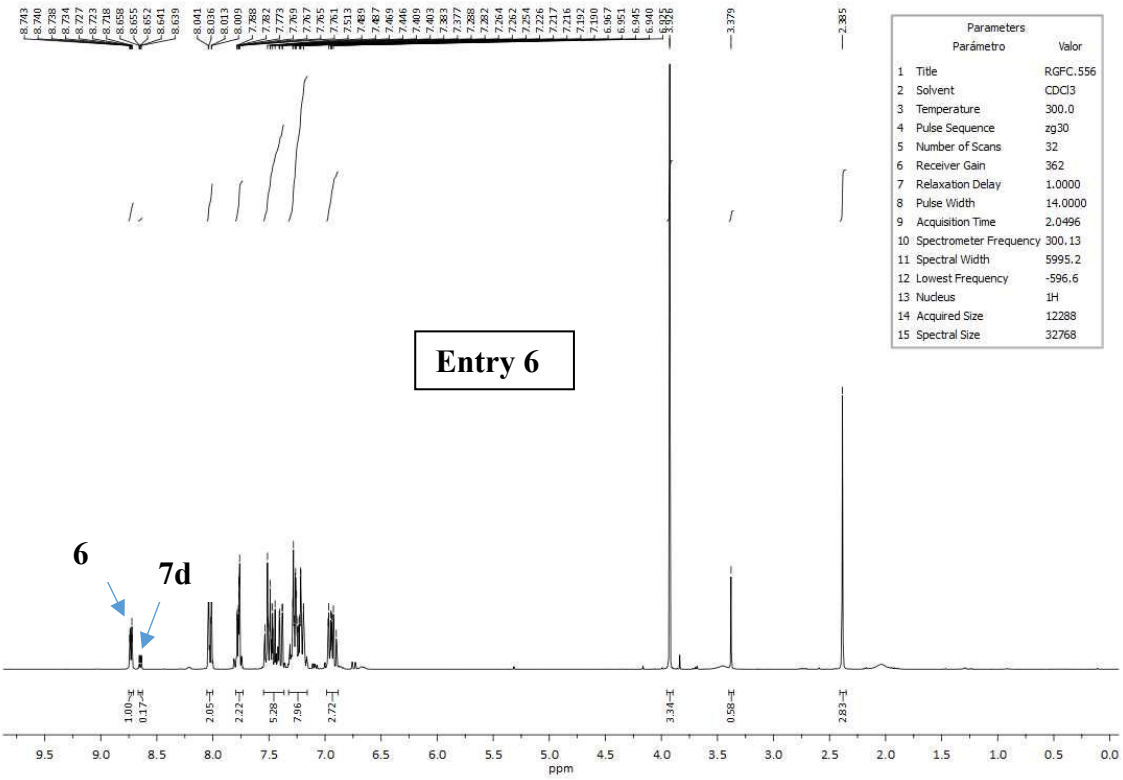

Figure S50: ^{1}H NMR spectrum (300 MHz, $CDCl_3$) of reaction collected in entry 6 of Table 7.

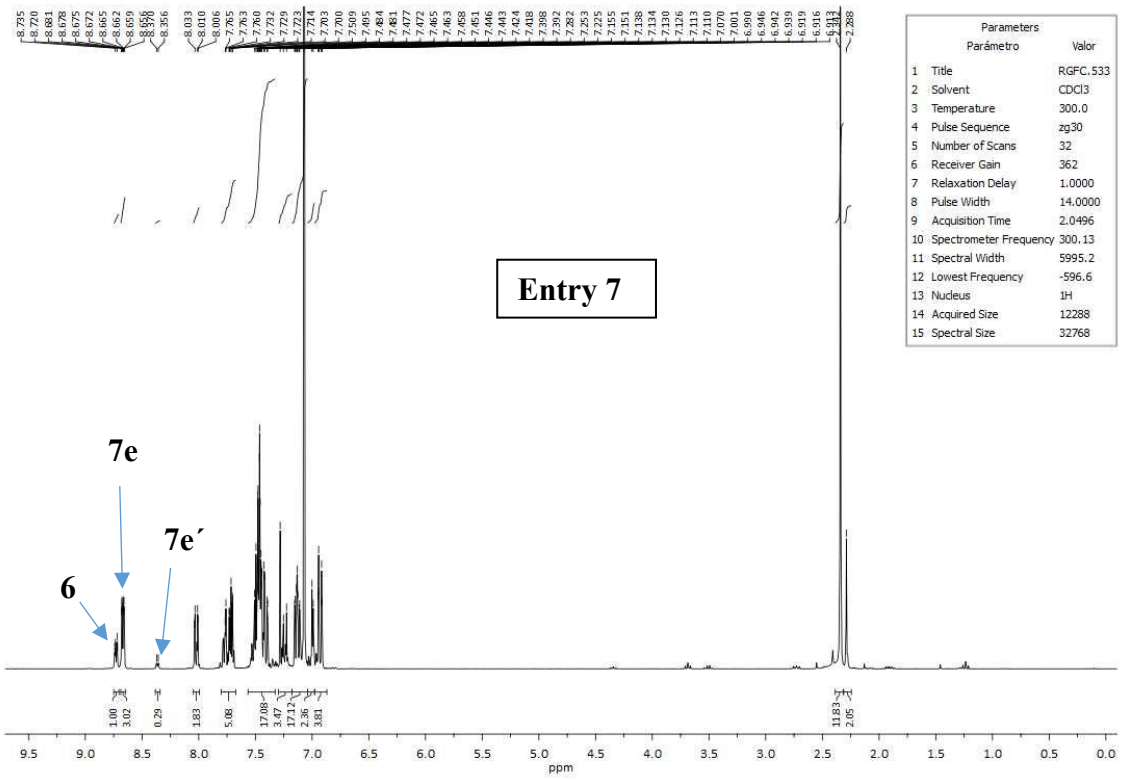

Figure S51: ^{1}H NMR spectrum (300 MHz, $CDCl_3$) of reaction collected in entry 7 of Table 7.

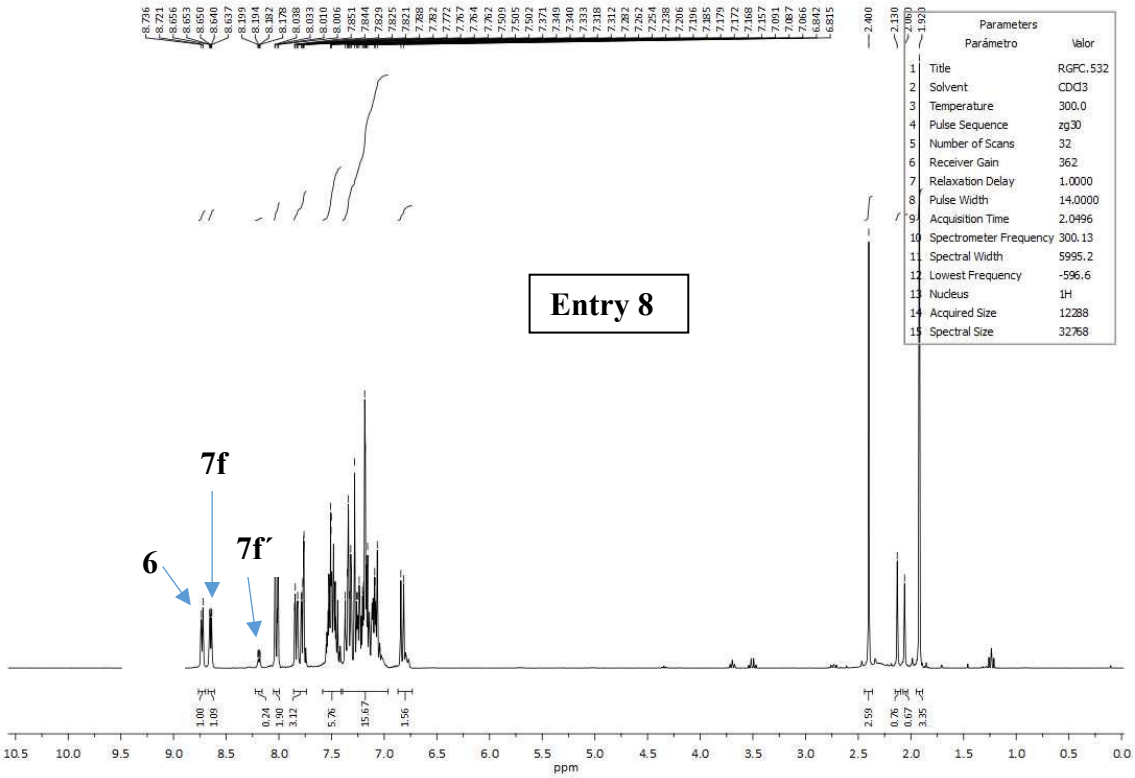

Figure S52: ^{1}H NMR spectrum (300 MHz, $CDCl_3$) of reaction collected in entry 8 of Table 7.

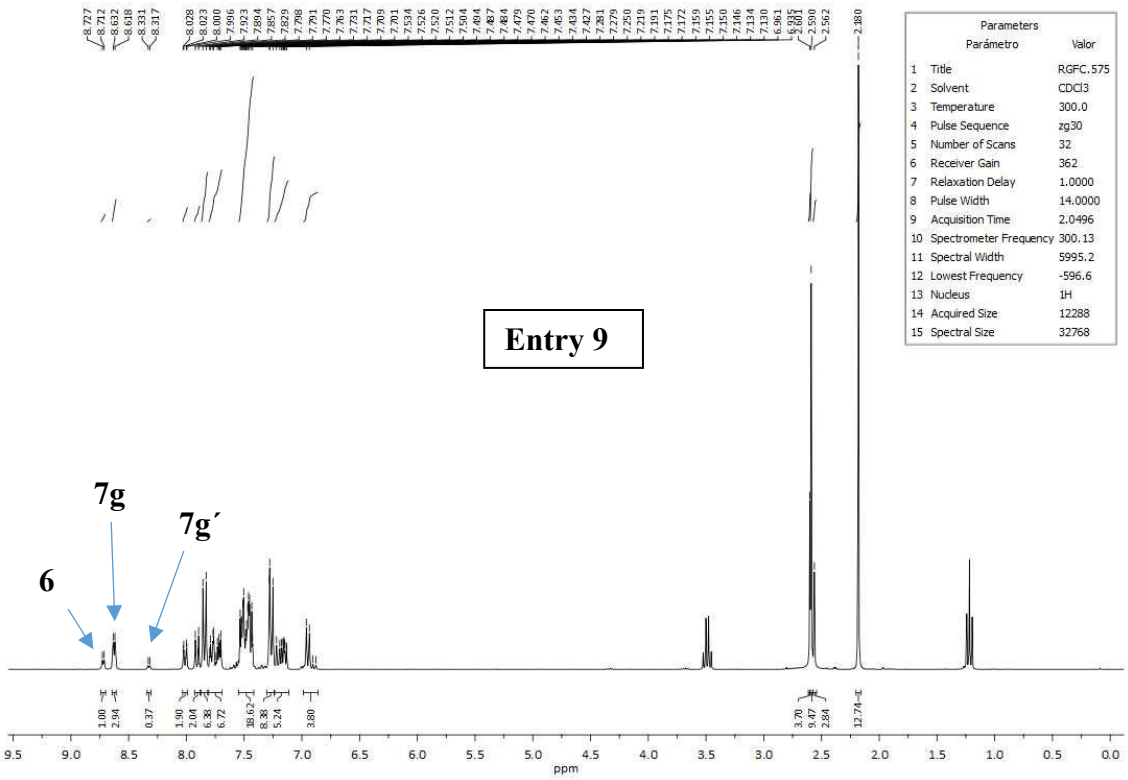

Figure S53: ^{1}H NMR spectrum (300 MHz, $CDCl_3$) of reaction collected in entry 9 of Table 7.

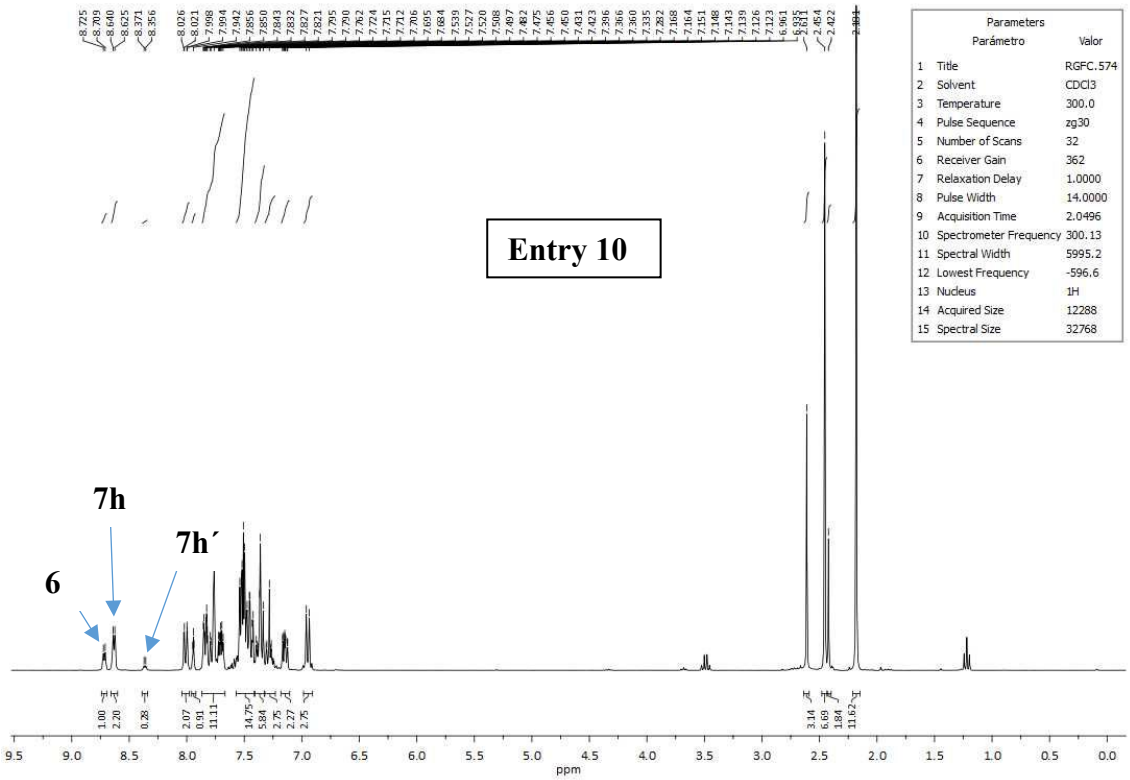

Figure S54: ^{1}H NMR spectrum (300 MHz, $CDCl_3$) of reaction collected in entry 10 of Table 7.

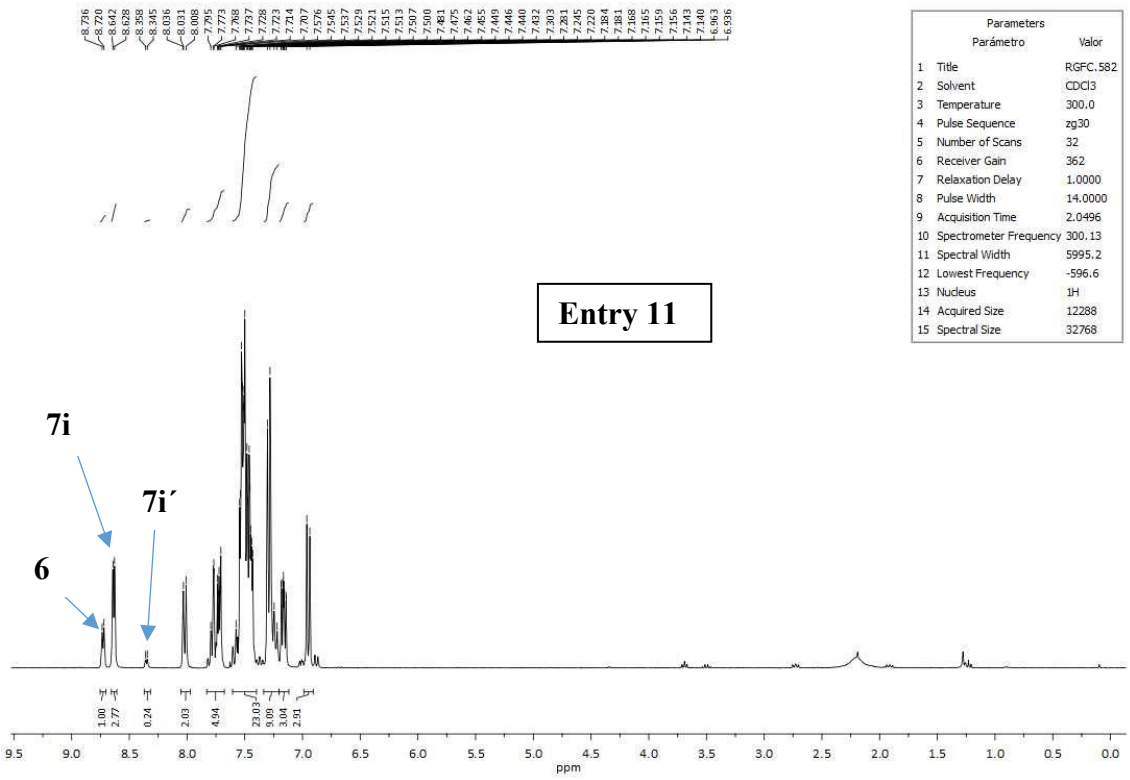

Figure S55: ^{1}H NMR spectrum (300 MHz, $CDCl_3$) of reaction collected in entry 11 of Table 7.